THE ROLE OF THE “ABCC6 PATHWAY” AND DIETARY PYROPHOSPHATE IN DYSTROPHIC CALCIFICATION

A THESIS SUBMITTED TO THE GRADUATE DIVISION OF THE UNIVERSITY OF HAWAI‘I AT MANOA IN PARTIAL FULFILLMENT OF THE REQUIREMENTS FOR THE DEGREE OF

MASTER OF SCIENCE

IN

MOLECULAR BIOSCIENCES & BIOENGINEERING

NOVEMBER 2018

BY: CHARNELLE B. JULIAN

Thesis Committee:

Dr. Olivier Le Saux, PhD, Chairperson

Benjamin Fogelgren, PhD

Takashi Matsui, MD, PhD

Jun Panee, PhD

ACKNOWLEDGMENTS

I would first like to thank my advisor, Dr. Olivier Le Saux, for giving me the opportunity to research and be a part of his lab family. Through the many challenges of graduate school, he always had an open door for advice and pushed me to be a better researcher and student. I especially appreciated how he understood the importance of making family a priority alongside research.

I would also like to thank Dr. Viola Pomozi. Her kindness and patience were apparent in all aspects of her work, including the time she invested in me as a mentor. Thank you for setting such a great example, teaching me numerous laboratory techniques, and always being available to answer my questions. She made my lab experience wonderful and positive. I would like to thank Janna for her friendship and countless hours spent performing vivarium procedures with me. The work she does to keep the lab running has not gone unnoticed and has been essential for the completion of my thesis.

I would also like to acknowledge my Molecular Biosciences and Bioengineering (MBBE) graduate chair advisor at the University of Hawai‘i at Manoa, Dr. Jon-Paul Bingham, for allowing me to be part of the MBBE program. His excellent organization as a graduate chair has made navigating the program a great experience. I would also like to thank my committee members, Dr. June Panee, Dr. Benjamin Fogelgren, and Dr. Takashi Matsui, for the time and expertise they have lent to my project. Also, thank you to the Ingeborg V.F. McKee Fund of the Hawai‘i Community Foundation and the National Institutes of Health for their financial support.

I want to express immense gratitude to my parents, boyfriend, Grace Group sisters, and friends for their constant prayers and support throughout my entire graduate school experience. This accomplishment would not have been possible without you. And, finally, thank you to the Lord for perfectly orchestrating this season of my life because it has been immeasurably more than anything I hoped for.

LIST OF ABBREVIATIONS

Acc	accelerated
ACDC	arterial calcification due to deficiency of CD73
ADP	adenosine diphosphate
AMP	adenosine monophosphate
ATP	adenosine triphosphate
ABC	ATP-binding cassette
AVS	Animal Veterinary Services
CALJA	calcification of joints and arteries
Ca^{2+}	calcium
cDNA	complimentary deoxynucleic acid
CFTR	cystic fibrosis transmembrane conductance regulator
CO_2	carbon dioxide
DNA	deoxyribonucleic acid
DCC	dystrophic cardiac calcification
ENPP1	ectonucleotide pyrophosphatase/phosphodiesterase 1
EtOH	ethyl alcohol
GACI	generalized arterial calcification of infancy
HCl	hydrochloric acid
IACUC	Institutional Animal Care and Use Committee
irr	irradiated
ip	intraperitoneal
JABSOM	John A. Burns School of Medicine

MRP6	multidrug resistance-associated protein 6
NBF	neutral buffered formalin
NT5E	ecto-5'-nucleotidase
PBS	phosphate-buffered saline
PO_4^{3-}	phosphate
Pi	inorganic phosphate
PPi	pyrophosphate
PXE	pseudoxanthoma elasticum
RNA	ribonucleic acid
RT-qPCR	quantitative reverse transcription PCR
TNAP	tissue non-specific alkaline phosphatase
TMDs	transmembrane domains
WT	wildtype

ABSTRACT

Soft tissue calcification occurs in pathologies such as atherosclerosis and diabetes and genetic disorders like pseudoxanthoma elasticum (PXE). PXE is caused by mutations in *ABCC6* and its symptoms include calcification in the skin, eyes, and cardiovascular tissues. ABCC6 is expressed primarily in the liver and kidneys and mediates the efflux of ATP. The released ATP is rapidly degraded by the ectocnucleotidases ENPP1 and NT5E into adenosine and pyrophosphate (PPi), with PPi being a potent inhibitor of calcification. Thus, ABCC6 is an upstream regulator of a pathway that modulates PPi production and adenosinergic signaling affecting ectopic calcification. The *Abcc6*$^{-/-}$ mice display calcification symptoms similar to human PXE patients in addition to an acute and inducible dystrophic muscle calcification phenotype. We hypothesize 1) the lack of Abcc6 lowers ATP efflux and influences the expression of *Enpp1* and *Nt5e,* thereby impacting plasma PPi levels and calcification susceptibility and 2) ABCC6 deficiency causes dystrophic calcification in cardiac tissues and skeletal muscle. The aims of this study were to 1) characterize the muscle calcification phenotype, 2) explore gene expression of the "Abcc6 pathway" and its molecular players, and 3) supplement PPi to counteract skeletal muscle calcification. Our inability to reproduce previous gastrocnemius calcification data for Aim 1 despite multiple trials and attempting protocol optimization led to the discovery of elevated levels of PPi in the rodent chow. Surprisingly, reversion to a low PPi diet did not restore the calcification phenotype and instead reduced calcium deposits in muscle tissues. The testing of an acceleration diet designed to enhance calcification was infructuous as it produced mineralization even in wild type mice. Our results demonstrated the impact that animal chow can have on

phenotypic outcome. Moreover, our data may provide an explanation for the phenotype variability in PXE patients and further suggested that dietary intervention to slow the progression of the calcification phenotype of PXE in patients may be possible. Gene expression studies showed positive correlation between the Abcc6 status and *Enpp1* and *Nt5e* mRNA levels in heart tissues. However, since we showed that PPi supplementation influences the expression of *Enpp1*, the presence of high levels of PPi in mouse chow probably negatively influenced our data. The Aim 3 experiments could not be completed as planned since we discovered elevated levels of PPi in the animal diet. However, results of specific Aim 1 provided some indications that indeed supplementation with PPi can effectively suppress dystrophic calcification in muscle tissues. Overall, the discovery of the elevated levels of PPi in the diet prevented us from achieving some of the goals of our specific aims and produced unanticipated but valuable data. Collectively, these studies have improved our understanding of the role of Abcc6 and PPi in the inhibition of soft-tissue calcification.

TABLE OF CONTENTS

ACKNOWLEDGMENTS **2**

LIST OF ABBREVIATIONS **3**

ABSTRACT **5**

LIST OF FIGURES **10**

CHAPTER 1: INTRODUCTION **12**

ABCC6 ..... **13**

Pathologic Calcification **15**

Pseudoxanthoma elasticum (PXE) **16**

Generalized Arterial Calcification of Infancy (GACI) **18**

Calcification of Joints and Arteries (CALJA) **20**

Mouse Models **20**

Calcification Phenotypes **21**

The Proposed "ABCC6 pathway" **23**

Inorganic Pyrophosphate (PPi) **24**

CHAPTER 2: MATERIALS AND METHODS **26**

Animals **26**

Survival Surgeries **27**

Myocardial Cryoinjury 27

Skeletal Muscle Cryoinjury 27

PPi Supplementation **28**

Histochemistry **28**

Alizarin Red 28

H&E 29

Quantification Assays **29**
Colorimetric Calcium Measurement 29
Pyrophosphate Measurement of Food 30
Molecular Biology Methods **30**
RNA Isolation 30
cDNA synthesis 31
Reverse Transcriptase Quantitative PCR (RT-qPCR) 31
Statistical Analysis **32**
CHAPTER 3: RESULTS **33**
Specific Aim 1: **33**
Hypothesis: 33
Preliminary Data **33**
Skeletal Muscle Calcification Phenotype 33
Approach and Significance: 35
Attempt to Optimize Cryoinjury Method to Induce Calcification **36**
Exogenous Sources of PPi 39
Testing the effects of the PPi (2920) diet on *Enpp1*$^{-/-}$ mice **42**
Reverting to low PPi Diet **43**
Acceleration Diet **44**
Specific Aim 2: **45**
Hypothesis: **46**
Approach and Significance **46**
Preliminary Data 46
Optimizing Gene Expression Analysis **46**
Gene Expression Results **47**

Changes in Gene Expression with the Acceleration Diet **50**

Specific Aim 3: **51**

Hypothesis: 51

Approach and Significance 51

PPi Through Diet **52**

CHAPTER 4: DISCUSSION AND FUTURE DIRECTIONS **53**

The unexpected consequences of dietary PPi on calcification **53**

The Acceleration diet may not be an appropriate tool for the *Abcc6*$^{-/-}$ mouse model **56**

A unique response to injury in the diaphragm **56**

Further molecular characterization of key players in the "ABCC6 pathway" **57**

Conclusion **58**

Literature Cited **60**

LIST OF FIGURES

Figure 1: The three-dimensional homology model of the ABCC6 protein. 14

Figure 2: PXE symptoms in the skin. 17

Figure 3: Cardiovascular and ocular PXE symptoms. 18

Figure 4: Severe calcification of cardiovascular and periarticular tissues in GACI. 19

Figure 5: Cryoinjury induces the DCC phenotype and causes increased cardiac calcium deposition. 22

Figure 6: The proposed ABCC6 pathway inhibits ectopic calcification. 23

Figure 7: The cryoinjured Abcc6$^{-/-}$ quadriceps (skeletal muscle) with more calcification than WT. 34

Figure 8: Calcium staining of Abcc6$^{-/-}$ tissues injured in survival surgeries. 35

Figure 9: Attempted optimization of cryoinjury protocol only marginally successful with increased calcium quantified in injured Abcc6$^{-/-}$ gastrocnemius but not visualized histologically. 38

Figure 10: The 2016 rodent diet with a significantly higher concentration of PPi compared to diet used prior to 2015, and nominal PPi content in drinking water. 41

Figure 11: The High PPi diet is linked to reduced Abcc6$^{-/-}$ mice vibrissae calcification. . 42

Figure 14: The Acc diet increased calcification in Abcc6-/- and WT mice. 45

Figure 15: Abcc6$^{-/-}$ livers with lower basal Enpp1 expression. 46

Figure 16: The largest change in gene expression occurs 3 days after injury. 47

Figure 17: There is positive correlation with Abcc6 in expression of Enpp1 and Nt5e in the heart on the high PPi diet and a trend of increased Enpp1 expression 3 days after injury. 49

Figure 18: Minimal conclusions could be drawn regarding the impact of the acceleration diet on Enpp1 expression in the heart and gastrocnemius. 50
Figure 19: No conclusions could be drawn regarding the impact of the high PPi diet on diaphragm Enpp1 expression.....51
Figure 20: PPi supplementation has a strong attenuate response in heart Enpp1 expression. 52
Figure 21: Dietary PPi appears to reduce calcification in Enpp1$^{-/-}$ mice(ttw) mice. 54
Figure 22: Radiation is not the source of increased PPi in the 2920 diet.....55
Figure 22: Calcification in the Abcc6$^{-/-}$ diaphragm with high PPi diet 37

CHAPTER 1: INTRODUCTION

Calcification

Calcium metabolism is a complex and closely regulated biological process that is usually associated with the formation of teeth and bones [1]. Calcium and phosphate (PO_4^{3-}) are the principal components of organized hydroxyapatite crystals ($Ca_{10}(PO_4)_6OH_2$). At physiological concentration, the concentrations of Ca^{2+} and PO_4^{3-} are near saturation and crystallization can occur readily. Because of this, the body employs several processes to ensure these ions are maintained at specific physiological concentrations and suggests plasma contains inhibitory factors that help regulate mineralization [2] [3].

Calcium plays a key role in cellular processes including hormone secretion, muscle contraction, and nerve conduction. It also acts as a secondary messenger that transmits extracellular information and signals to the interior of the cell. Due to its many functions, the physiologically active free ionic form of Ca^{2+} in the plasma is carefully maintained in a narrow range (between 1.0 and 1.3 mM) with the help of ion channels, certain organelles, and specialized transporters [4]. Most of the body's calcium is located within the bones and teeth while the rest exists in plasma as a free ionic species, associated with serum proteins, or bound to lower-molecular weight anions. Phosphate is also essential for various physiological processes and, like calcium, its physiological levels are tightly regulated. Phosphate is important for bone formation and for its role in energy formation with phosphate being an essential component of the adenosine triphosphate (ATP) molecule. The body uses phosphate derived compounds

in many biological activities such as cell signaling, enzyme function, and waste excretion [5] [4].

ABC Transporters

ATP-binding cassette (ABC) transporters are an important class of membrane-bound protein pumps. The human proteome consists of 48 ABC proteins, which are grouped into seven subfamilies from A to G based on sequence similarity. These proteins may function as unidirectional (efflux) pumps that hydrolyze ATP to export many molecules from the cytoplasm into the extracellular space, and their presence in the intestinal tract and blood brain barrier is instrumental for removing toxic molecules [6]. These proteins can also regulate nearby ion channels and function as an ion channel [3].

ABC proteins have the same general structural features. The proteins are made up of two transmembrane units, and each unit is comprised of six membrane-spanning α-helices that are connected to two intracellular ATP-binding subunits just beneath the plasma membrane. The binding of ATP induces a conformational change that exposes a substrate-specific binding site. Once ATP is hydrolyzed, ADP dissociates and the transporter returns to its original conformation [6].

ABCC6

The ABCC subfamily has 12 members with the majority of them acting as active transporters [7]. This subfamily of proteins notably includes ABCC7 (also known as CFTR) which is associated with cystic fibrosis. ABCC6 is also known as multidrug resistance-associated protein 6 (MRP6) and *ABCC6* is located at 16p13.11 on chromosome 7. The functional gene spans 75 kD and consists of 31 exons. The ABCC6

/MRP6 protein is made up of 1503 amino acids and functions as an organic anion transporter [8] [9] . ABCC6 is primarily expressed in the liver with lower levels of expression in the kidney, though many other cell types also express detectable levels of the protein [10] [11].

As for all other ABC proteins, the ABCC subfamily of proteins consists of the core structure of two nucleotide-binding domains and two transmembrane domains (TMDs) with six transmembrane helices. ABCC1, 2, 3, 6, 8, 9, and 10 have two unique structural features located N-terminally: the TMD0 domain comprised of five membrane spanning helices that connects with the other transmembrane helices via an intracellular loop (L0) [7]. Homology models (***igure 1***) depict ABCC6 with the ABC domains located in close proximity to each other, forming a head-to-tail dimer.

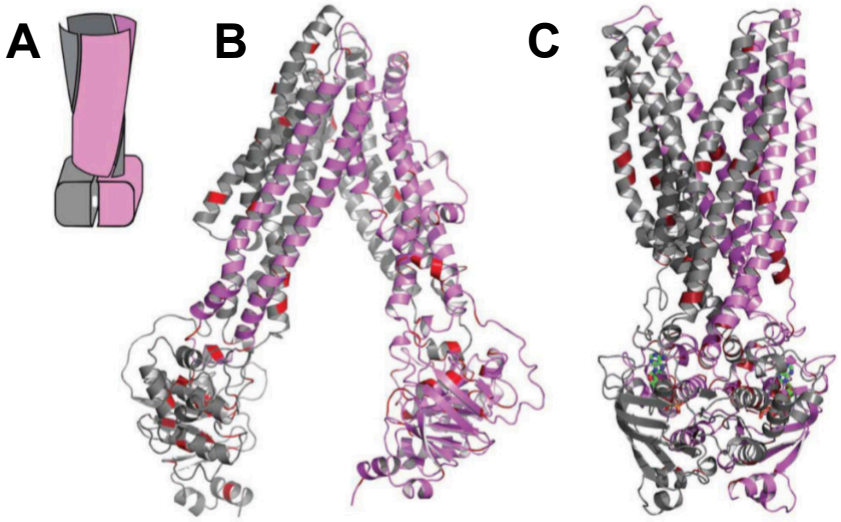

Figure 1: The three-dimensional homology model of the ABCC6 protein.

A) *Schematic representation of domain swapping of ABC proteins* ***B)*** *Three-dimensional model of the outward facing conformation* ***C)*** *Three-dimensional nucleotide-free confirmation.*

Pathologic Calcification

Pathological (ectopic) calcification is characterized by the deposition of hydroxyapatite crystals in the soft tissues. Dystrophic calcification is a type of pathologic calcification that occurs specifically in response to injury. For example, the tissue damage that occurs during surgical procedures initiates an inflammatory response that occasionally results in calcification of the soft tissues. Most soft tissue calcification may be visualized with X-rays [12]. The presence of dystrophic calcification increases the risk for developing heterotopic ossification, the formation of bone outside of its normal place [12].

Pathologic calcification is also common to several naturally occurring pathologies such as diabetes, renal failure, hypercholesterolemia, and certain genetic disorders [13]. The small and middle-sized arteries of the cardiovascular system are especially susceptible to calcification and are associated with symptoms including, but not limited to, diminished peripheral pulses, hypertension, and atherosclerosis.

The delicate balance of calcium metabolism is influenced by multiple internal and external factors such as aging, tissue injury, diet, chronic renal insufficiency, and diabetes [14]. Genetic risk factors include mutations in genes that cause the heritable diseases pseudoxanthoma elasticum (PXE) and generalized arterial calcification of infancy (GACI), where pathologic calcification is the most detrimental side effect, as well as calcification of the joints and arteries (CALJA), formally known as arterial calcification due to deficiency of CD73 (ACDC). In depth studies of these diseases have provided a better understanding of how the regulation of specific genes may contribute to biological

calcification. The wide range of complications associated with pathologic calcification make it an important area of research.

In contrast to dystrophic calcification, metastatic calcification results from elevated extracellular levels of calcium (hypercalcemia) that exceed the normal homeostatic levels [12]. Mineralization may occur in cells and extracellular matrix components like collagen, basement membranes, elastic fibers, and arterial walls. Metastatic calcification is linked to pathologies such as renal failure and hyperparathyroidism and on X-ray appears as fine, diffuse speckles throughout soft tissue [12].

Pseudoxanthoma elasticum (PXE)

Mutations in *ABCC6* have been linked to PXE. The prevalence of PXE is known and is estimated at 1 in 25,000 to 1 in 50,000 [15]. In 2000, positional cloning experiments linked loss-of-function mutations in both alleles of *ABCC6* directly to the pathogenesis of pseudoxanthoma elasticum [16]. Up to now, more than 400 mutations have been identified with disease-causing changes resulting from single nucleotide substitutions and small and large deletions [17]. The most common loss-of-function mutations identified in PXE are p.R1141X (20-30) and c.EX23_29del [18].

PXE is an autosomal recessive disease of the connective tissue causing progressive peripheral ectopic calcification of the skin, eyes, and arteries. Presently, there are no effective therapies for PXE [11]. The hallmark symptom of PXE is the formation of yellowish papules in the skin that eventually coalesce to form distinct plaques (Figure 2A). The flexor surfaces of the body, such as the axilla (Figure 2B) and groin, develop redundant folds due to increased skin laxity and results in a prematurely

aged appearance (Figure 2) [19] [20]. The inelasticity of the skin can be visualized by histopathologic analysis of the skin lesions of PXE patients (Figure 2C), which depict mineralization of the dermal collagen fibers [19].

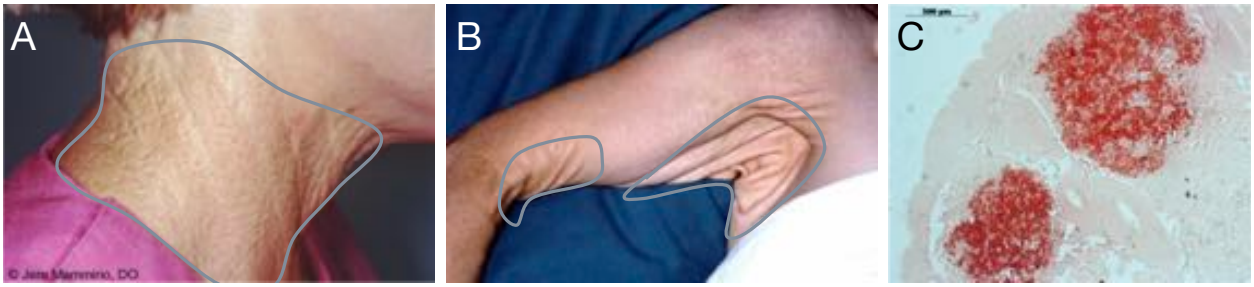

Pomozi et al, 2017

Figure 2: PXE symptoms in the skin.

The flexor surfaces such as the neck and axilla exhibit distinct plaques ***(A,B)****. Histopathological analysis of the skin confirms calcification (scale 500 μM)* ***(C).***

The eyes and cardiovascular tissues are also affected by calcification and are responsible for the morbidity of PXE [17]. Examination of the fundus shows angioid streaks, which represent breaks in the Bruch's membrane (Figure 3B). These breaks may lead to choroidal neovascularization, hemorrhages (Figure 3C), and eventually loss of central vision. Cardiovascular tissues are affected with early onset of atherosclerosis [7]. The hardening of the leg arteries (Figure 3D) causes intermittent claudication while calcification of the coronary artery increases risk for myocardial infarction [19]. *ABCC6* has also been classified as a potential genetic risk factor in coronary artery disease (CAD) [14]. Other complications include hypertension, arterial insufficiencies in the extremities, and gastrointestinal hemorrhages [20].

The clinical manifestations of PXE are highly varied and the severity of symptoms differs extensively among families with no clear genotype-phenotype correlation. This phenotypic heterogeneity of PXE adds a layer of complication when

studying the disease. Diagnosis can be difficult since symptoms typically do not appear until puberty. Additionally, establishing the correct diagnosis is difficult since the clinical conditions are identical to pathologies of other disorders [19].

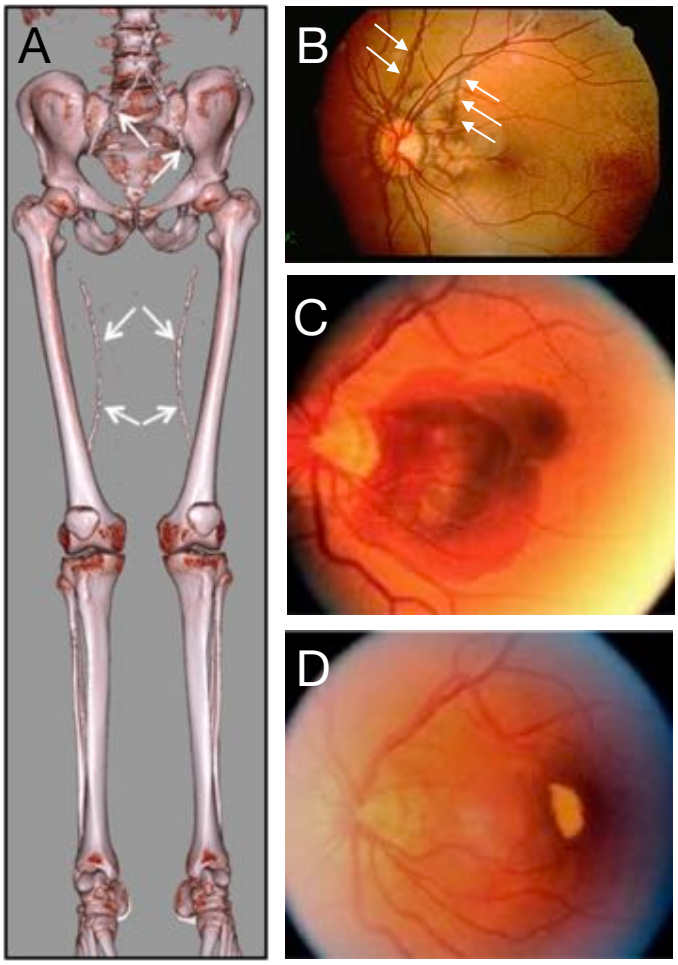

Figure 3: Cardiovascular and ocular PXE symptoms.

*Calcification may occur in major arteries such as the major iliac arteries (white arrows) in the leg **(A)**. Ocular symptoms result from calcification of the Bruch's membrane (white arrows) **(B)** that in turn causes retinal hemorrhaging **(C)** and eventually leads to macula scarring and a loss of central vision **(D)**.*

Generalized Arterial Calcification of Infancy (GACI)

The other genetic disease resulting, in part, from *ABCC6* mutations is a rare autosomal recessive disorder called generalized arterial calcification of infancy (GACI). It is characterized by severe pathologic calcification of the arterial media and intimal layers and loss of integrity of the elastic fibers, ultimately culminating in severe arterial stenosis (

Figure 4) [1]. Other symptoms include congestive heart failure, hypertension, and myocardial ischemia. Most patients die within the first six months of life, while some others treated with bisphosphonates had better outcomes.

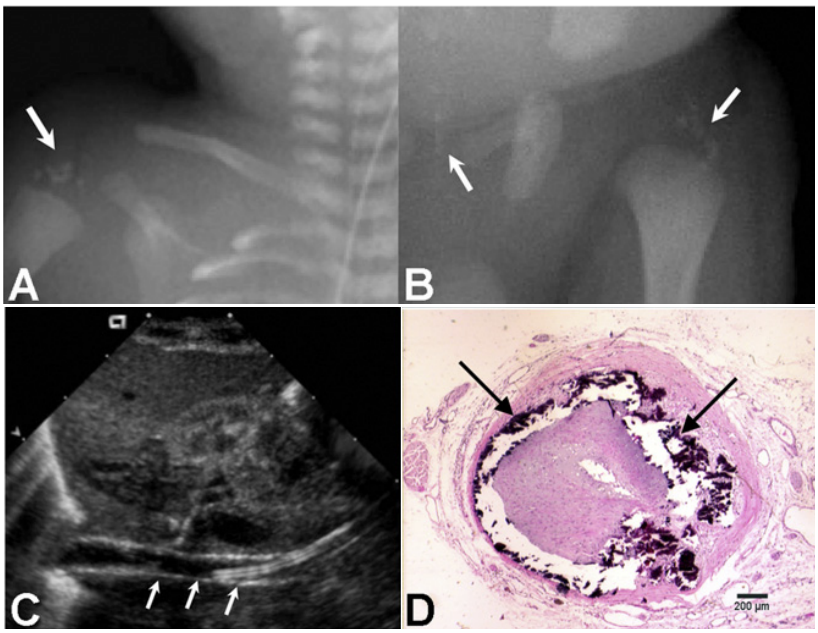

Nitschke *et al*, 2012

Figure 4: Severe calcification of cardiovascular and periarticular tissues in GACI.

X-ray visualization of periarticular calcification (white arrows) ***(A,B)****. Aortic calcification seen on ultrasound (white arrows)* ***(C)*** *and with H&E staining (black arrows)* ***(D)****.*

A loss-of-function mutation in *ENPP1* accounts for 75% of the GACI cases. *ENPP1* encodes for an ectonucleotide pyrophosphatase that preferentially hydrolyzes ATP to form PPi, and therefore plays an important role in bone mineralization [21]. Interestingly, a significant portion of patients with GACI also carried *ABCC6* mutations while some PXE patients only carry *ENPP1* mutations [22]. This study showed that patients with GACI had PXE-like symptoms such as angioid streaks and identical skin lesions. These findings were the first indication that ENPP1 and ABCC6 are linked through a molecular pathway contributing to calcification [1].

Calcification of Joints and Arteries (CALJA)

The disease CALJA is characterized by adult onset calcification of the lower extremities in the iliac, femoral, and tibial arteries, as well as in the hand and foot capsule joints. It is an autosomal recessive condition caused by mutations in *NT5E*, which encodes the adenosine-generating ecto5'-nucleotidase that catalyzes the conversion of adenosine monophosphate (AMP) into adenosine and inorganic phosphate (Pi) [23]. Identifying mutations in *NT5E* was the first indication that altered purinergic signaling could modulate calcification from insufficient adenosine production and activation of tissue non-specific alkaline phosphatase (TNAP/*ALPL*) [24]. Indeed, CALJA is caused by enhanced PPi degradation due to the activation of TNAP [25, 26], which degrades PPi into Pi, an activator of calcification.

Mouse Models

Use of *Abcc6*$^{-/-}$ mice has been instrumental in the study of PXE. Past studies demonstrate the phenotype of *Abcc6*$^{-/-}$ mice duplicates rather faithfully the human PXE pathology, though there are divergent areas of mineralization between mice and humans. Starting shortly after weaning, both male and female mice develop progressive calcification of renal vessel walls without affecting renal function. In older animals, elastic fibers in the vessel walls of other large and medium-sized arteries develop calcium deposits, mirroring the cardiovascular pathologies of PXE patients [20]. Unlike human PXE patients, mice did not show significant calcification of the dermis or flexor areas. Calcification of the ocular Bruch's membrane is comparable to their human counterparts, though it's unclear if the mice develop angioid streaks, retinal hemorrhages, and/or lose vision. Remarkably, mineralization in mice is first detected in vibrissae, a connective tissue capsule that surrounds the hair bulb of each vibrissa in muzzle skin, a tissue not present in humans [27]. The vibrissae calcification serves as a useful marker of disease progression in *Abcc6*$^{-/-}$ mice and is first detectable at 5 to 6 weeks of age, increasing progressively with time [19]. Overall, these similarities in the calcification phenotype between mice and humans make *Abcc6*$^{-/-}$ mice an excellent model for investigating PXE.

Calcification Phenotypes

Calcification associated with ABCC6 deficiency can be subdivided into two distinct phenotypes: a chronic and passive manifestation and an acute inducible phenotype. The main PXE phenotype is characterized by long-term, chronic calcification

affecting primarily elastic fibers within the extracellular matrix of skin, arteries, and retina. This phenotype is progressive and irreversible [18] [28].

The other phenotype is referred to as dystrophic cardiac calcification or DCC. Several commercially available strains of mice (C3H/HeJ, DBA/2J, and 129S1/SvJ) were described years ago [29] as developing severe dystrophic calcification after cardiovascular injuries, ischemia, or high fat diets [30]. Examination of F_2 intercrosses of C57BL/6J and susceptible animals C3H/HeJ mice (also called C3H) identified a major susceptibility locus, *Dyscalc1*, on chromosome 7 [31] [32]. Within this locus, a single specific *Abcc6* mutation resulted in a constitutive decrease in Abcc6 protein levels in liver and is directly responsible for the DCC phenotype [10, 29]. Additional minor *Dyscalc* loci were also identified (*Dyscalc2* to *4*) and mapped to chromosomes 4, 12, and 14. These modifier loci affect the penetrance and expression of the DCC phenotype [30]. DCC occurs independently of calcium and phosphate homeostasis.

Unlike passive PXE-like calcification, DCC is acute, develops over a very short period of time, and affects all muscular tissues including skeletal muscle (
). Furthermore, DCC occurs intracellularly, seemingly initiated within mitochondria. Therefore, the chronic and acute molecular pathways leading to calcification probably share a mechanism of initiation (Abcc6 deficiency) but their progressions are distinct [14]. The main characteristics of DCC, inducibility and rapid development (within days), have been effectively used by Dr. Le Saux's laboratory as a convenient research tool to expand our understanding of ABCC6 and to develop strategies to treat PXE patients (
) [14, 33, 34]. In this research project, we focused on the molecular characteristics of DCC.

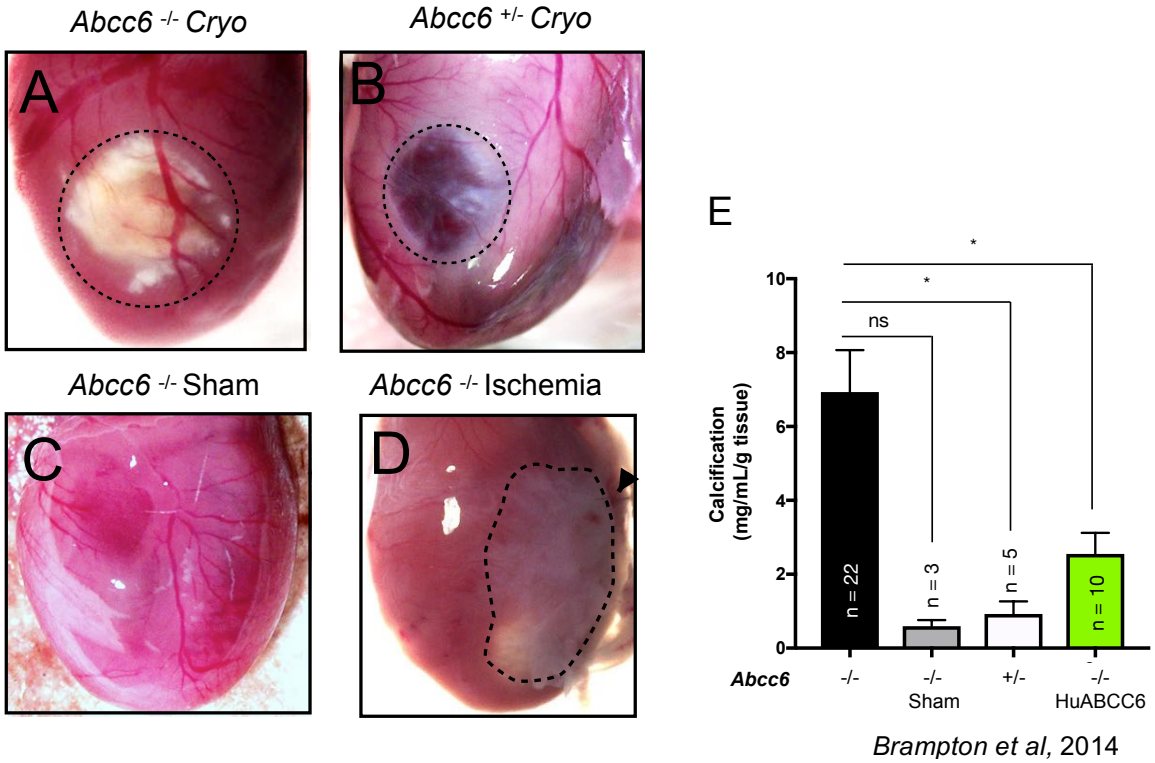

Figure 5: Cryoinjury induces the DCC phenotype and causes increased cardiac calcium deposition.

*A robust calcium deposition in Abcc6$^{-/-}$ mice induced by freeze-thaw injury in 2-4 days **(A,E)**. The Abcc6$^{+/-}$ mice **(B,E)** and Abcc6$^{-/-}$ sham control **(C,E)** did not show abnormal calcification. The green bar (**E**) represents the transient expression of Human ABCC6 (HuABCC6) in liver, which significantly reduced cardiac calcification.*

The Proposed "ABCC6 pathway"

An "ABCC6 pathway" has been proposed with several key molecular players. ABCC6 seems to initiate molecular processes leading to pyrophosphate generation, which prevents abnormal calcification [34]. In this model (

Figure 6), ABCC6, located on the basolateral side of hepatocytes (and other cell types) mediates the cellular efflux of ATP. The AMP indirectly inhibits calcification by inhibiting tissue-nonspecific alkaline phosphatase (TNAP) synthesis. The absence of TNAP prevents the breakdown of PPi into Pi, which would otherwise activate soft-tissue calcification [26].

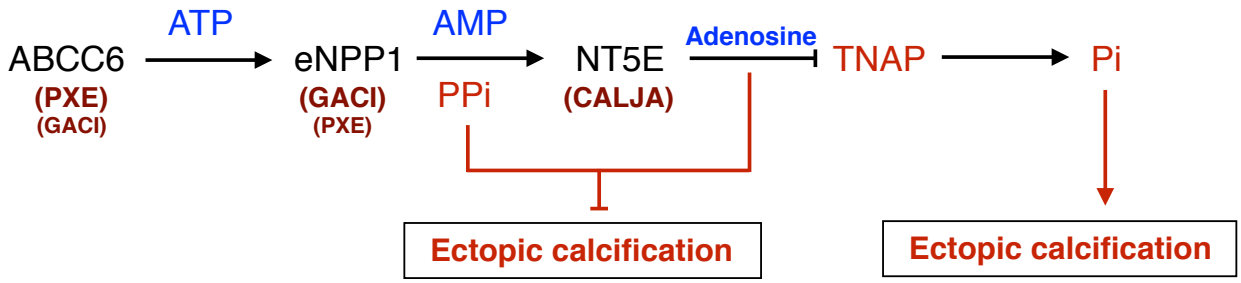

Pomozi et al, 2017

Figure 6: The proposed ABCC6 pathway inhibits ectopic calcification.

ABCC6 facilitates the cellular efflux of ATP from liver and other tissues/cells, which is quickly converted to pyrophosphate (PPi), a potent inhibitor of mineralization. Decreased plasma PPi levels cause calcification in PXE and GACI. NT5E activity leads

to adenosine production, which inhibits TNAP expression. TNAP otherwise degrades PPi into inorganic phosphate (Pi), an activator of calcification.

Inorganic Pyrophosphate (PPi)

In humans, inorganic pyrophosphate (PPi) is found mainly in body fluids, but is also present in blood cells, calcified tissues, bone, and teeth. Inorganic pyrophosphate (PPi) is a by-product of many *in vivo* biosynthetic reactions. There are various PPi forming reactions in multiple regions of metabolism that involve proteins, carbohydrates, lipids, and nucleic acids [2]. These PPi-producing reactions include but are not limited to: synthesis of aminoacyl-tRNA, activation of carboxylic acids, protein degradation and modification, and nucleotide synthesis [2].

PPi is essential to calcium metabolism because it is a known inhibitor of calcification and works by preventing the crystallization of Ca^{2+} and PO_4^{3} [35]. Early *in vivo* and *in vitro* studies showed that hydroxyapatite crystals coated with PPi grew and dissolved much slower compared to controls [2]. Additionally, PPi inhibited the conversion of amorphous calcium into crystalized hydroxyapatite [2]. Conversely, alkaline phosphatases promote calcification by hydrolyzing PPi into inorganic phosphate (Pi) that can then form hydroxyapatite crystals with Ca^{2+}.

Previous studies in our laboratory characterized the structural and functional consequences of PXE-causing mutations in ABCC6. Three possible consequences were identified: 1) transport deficiency due to inability to use ATP, 2) altered protein folding and stability, causing the protein to be retained intracellularly, and 3) reduced trafficking efficiency but with normal *in vitro* transport activity [37]. Consequently, the missense *ABCC6* mutations studied all resulted in a loss of the physiological function,

thus providing a possible explanation for the lack of genotype-phenotype correlation in PXE. *In vitro* assays further confirmed that most of the mutants had abnormal cellular localization, where the ABCC6 protein failed to reach the plasma membrane in cultured cells and mouse liver. This confirms that PXE is not caused by a lack of ABCC6 in the tissues, but instead by the absence of the PPi it effluxes into circulation.

The levels of PPi in circulation became a topic of interest once ABCC6 was shown to efflux ATP, which is subsequently degraded into PPi at the cell surface. Generally, ATP is considered to stay inside living cells, but has been shown to exist in extracellular fluids. It is thought that ATP may enter the plasma after being excreted from blood platelets undergoing degranulation, via synaptic vesicles, and from smooth muscle cells through mechanisms not yet understood [2].

The link between ABCC6 and plasma PPi was supported by experimental evidence as Abcc6$^{-/-}$ mice have plasma PPi levels ~40% that of WT mice. Moreover, PXE patients present similarly lowered plasma PPi concentrations (~2.5 fold lower) as compared to healthy individuals [11] [36]. This suggests that ABCC6 accounts for approximately 60% of the PPi plasma levels in mice and humans [33]. Taken altogether, the proposed pathway (

Figure 6) and experimental evidence links decreased levels of plasma PPi to pathological calcification.

CHAPTER 2: MATERIALS AND METHODS

Animals

The *Abcc6*^{tm1JfK} mice (referred to in this study as *Abcc6*$^{-/-}$ mice) were developed by targeted ablation of the mouse *Abcc6* gene. These mice were made on the 129S1/SvImJ background and backcrossed on C57BL/6J background >10 times [27]. Inbred C57BL/6 and C3H/He strains were purchased from Charles River (Sulzbach-Rosenberg, Germany) [38]. The congenic strains were bred at the John A. Burns School of Medicine (JABSOM) Vivarium. The outset (C57BL/6 × C3H/He) F1 male mice were backcrossed to female C57BL/6 mice. Selected progeny were further backcrossed to female C57BL/6 mice for nine more generations with the aim to preserve (C57BL/6 × C3H/He) heterozygosity on proximal chromosome 7. DNA was isolated from each F_2 animal and genotyped using microsatellite markers D7Mit56, D7Mit247, D7Mit229, D7Mit82, D7Mit31, D7Mit40, and D7Mit33 [32]. Brothers and sisters were mated to produce a chromosome segment with homozygous alleles of the susceptible donor strain C3H/He. Throughout the entire experiment, all animals had free access to water and the standard rodent diet Altromin 1324 chow. The accelerated diet (Acc) contains specific mineral modifications to induce calcification in the *Abcc6*$^{-/-}$ mouse model. In comparison to the standard rodent diet, the Acc diet has a 2-fold increase in absorbable phosphorus (from 0.43% to 0.85%), a 22-fold increase in vitamin D3 (from 4.4 IU/g to 100 IU/g), and a decrease in calcium (from 1.0% to 0.4%) and magnesium (from 0.22% to 0.04%). Mice were maintained with a 12-hour light and dark cycle. The animal studies were approved by the Institutional Animal Care and Use Committee (IACUC) of JABSOM.

Survival Surgeries

Myocardial Cryoinjury

The WT and *Abcc6*$^{-/-}$ mouse strains ranging from 2-12 months in age underwent myocardial freeze-thaw injury. Mice were anesthetized with 5% isoflurane through nasal inhalation for 3-5 minutes then maintained at 3% throughout the procedure. A vertical incision was made to the midline of the abdomen through the skin, abdominal muscles, and peritoneal wall. The left lobe of the liver was lifted gently to visualize the beating heart through the translucent diaphragm. The probe (5 mm in diameter) was first cooled in liquid nitrogen for approximately 2 minutes and then gentle pressure was applied through the diaphragm to the heart for 10 seconds. The incision was closed in layers, starting with the abdominal muscle layer closure using 6.0 silk suture material and discontinuous sutures. Next the skin layer was closed using the same suture material and continuous sutures. The mice were sacrificed using carbon dioxide at either 3 or 7 days post-surgery [14].

Skeletal Muscle Cryoinjury

Mice ranging in age from 2-12 months from both WT and *Abcc6*$^{-/-}$ mouse strains underwent gastrocnemius (calf muscle) freeze-thaw injury. Mice were anesthetized with 5% isoflurane through nasal inhalation for 3-5 minutes then maintained at 3% throughout the procedure. While mice were positioned on their abdomens, an 8-mm incision was made through the skin and forceps were used to expose the underlying muscle. A single suture was made directly into the muscle using 6.0 suturing material. The probe (5 mm in diameter) was first cooled in liquid nitrogen for approximately 2

minutes, then gently pressed directly onto the suture for 30 seconds. The skin layer was closed using 6.0 suturing material and continuous sutures. The mice were sacrificed using carbon dioxide at 3 or 7 days post-surgery.

PPi Supplementation

PPi was purchased from Sigma-Aldrich (St. Louis, MO) as tetrasodium decahydrate salt. Based on a previous study [28], 100 mg/kg per day of PPi in 0.9% saline solution was administered to mice via intraperitoneal (ip) injection. Injections were initiated 24 hours before induction of DCC via cryoinjury and daily thereafter until euthanasia. Control animals received injections of saline. For the experimental groups of mice testing the effect of PPi on chronic calcification, the animals were weighed every week and the volume injected was adjusted accordingly. For control experiments, groups of mice were treated in parallel with saline injections. Cardiac and gastrocnemius tissues were harvested at day 7 after injury, as described above [34].

Histochemistry

Alizarin Red

For histochemical staining, the mice were euthanized by CO_2 asphyxiation either 3 or 7 days post cryoinjury depending on the procedure chosen. The diaphragm, peritoneal muscle, sutured abdominal skin, control and injured heart, and control and injured gastrocnemius muscle were fixed in 10% neutral buffered formalin (NBF) overnight, then stored in 70% EtOH at 4°C prior to paraffin embedding. Paraffin sections (5 μM thick) were stained with Alizarin Red S solution (Sigma, St., Louis MO) for 5 minutes and mounted using Permount (Fisher Scientific, Waltman, MS). Images were

collected using an Axioscope 2 fluorescent microscope (Zeiss, Thornwood, NY) and sections from each treatment group were visualized for calcium deposition [14].

H&E

The tissue samples for H&E staining were harvested in parallel with the Alizarin Red staining samples and stored overnight in 10% neutral buffered formalin (NBF) as described above. The biopsy specimens were embedded in paraffin and the sections (5 μM thick) were stained with hematoxylin and eosin and mounted using Permount (Fisher Scientific, Waltman, MS).

Quantification Assays

Colorimetric Calcium Measurement

The amount of calcium mineralization in the tissues was quantified using a colorimetric assay [39]. This assay directly measures the amount of calcium within excised tissue, and is normalized to the weight of the dry tissue. Excess tissue calcium (above background levels) reflects mineralization. For hearts, the atria were removed and only the ventricular area was used. For gastrocnemius muscle samples, the injured part of the muscle was distinguished from the uninjured parts with the single suture positioned at the time of injury and selectively excised. Heart and muscle tissue were placed in 0.15N HCl and incubated at room temperature for 48 hours. Samples were centrifuged at 13,200 rpm, and the total calcium content of the HCl supernatant was measured using the Calcium Liquicolor Kit (Stanbio, Boerne, TX) by measuring absorbance at 550 nm. The amount of calcium was normalized to the total dry tissue

weight before mincing. The calcium values were quantified against a known standard and expressed in μg/dL per milligram of tissue [18].

Pyrophosphate Measurement of Food- viola uses different protocol

PPi was extracted from 2.5 g of grounded chow in 15 ml of sterile Milli-Q water. The sample was agitated at 4˚C overnight then centrifuged. PPi was measured from the supernatant. The kit uses p-nitrophenyl phosphate as substrate, which is converted into colored p -nitrophenol measured by optic density at 405 nm. Units of alkaline phosphatase activity correspond to mmol of p-nitrophenol/mL per minute. ATP was measured in perfusion samples, as previously described, and in plasma using the Promega, G8230 BacTiter-Glo Microbial Cell Viability Assay from Promega (Madison, WI).

Molecular Biology Methods

RNA Isolation

Total RNA was extracted from tissue samples ranging in weight from 25-30 mg. Tissues were harvested and placed in RNAlater overnight, then weighed and placed into 50 μL of 1X PBS. Tissues were minced and digested in 500 μL of Trizol for 5 minutes, then 100 μL of chloroform were added. Samples were centrifuged for 15 minutes at 12,000 g at 4°C. The colorless supernatant was separated and total RNA was extracted using the RNeasy kit (Qiagen Inc., Valencia, VA).

cDNA synthesis

RNA was converted into first-strand cDNA using the SuperScript III First-Strand synthesis kit with random hexamers (ThermoFisher, Waltham, MA). The extracted RNA was combined with the appropriate amount of RNase-free water to obtain a concentration of 200 ng/μL. Next, 1 μL of RNAse free water, 1 μL of primer, and 1 μL of annealing buffer was added to each reaction. The samples were incubated at 65°C for 5 minutes then 4°C for 1 minute. 10 μL of 2X First-Strand Reaction Mix and 2 μL of SuperScript III Enzyme Mix were added and the samples were incubated for 5 minutes at 25°C, 50 minutes at 50°C, 5 minutes at 85°C, and 4°C forever. Samples were stored at -20°C until needed for RT-qPCR.

Reverse Transcriptase Quantitative PCR (RT-qPCR)

The RT-qPCR was carried out using the Applied Biosystems StepOnePlus RT-PCR system and the Design Wizard StepOne software (Applied Biosciences Inc., Foster City, CA). The levels of expression of mouse *Enpp1* (Life Technologies, Mm01193761_m1) *Nt5e* (Life Technologies, Mm00501910_m1)*, Abcc6* (Life Technologies, Mm01202683)*,* and reference gene *Gapdh* (Life Technologies, Mm99999915) were detected using commercially available T

aqMan probes (Applied Biosciences Inc., Foster City, CA). The StepOne software pre-determined the volume of each reagent needed to achieve appropriate concentrations and quantities for each reaction. First, the samples were prepared by combining RNAse free water and the cDNA stock solution of each sample in microcentrifuge tubes to achieve a concentration of 150 ng/μL. Next, the reaction mix

was made using TaqMan Mastermix, RNAse free water, and the appropriate TaqMan probe Assay Mix. The reactions were arranged in accordance with the plate layout made with StepOne Design Software. Each sample contained 59.4 μL of reaction mix and 6.6 μL of sample for a final volume of 65 μL. The negative control reactions contained 39.6 μL of reaction mix and 4.4 μL of RNAse free water to a final volume of 44 μL. Lastly, 20 μL of each sample was pipetted into the appropriate wells to make triplicates.

The samples were placed Applied Biosystems StepOnePlus RT-PCR system (Applied Biosciences Inc., Foster City, CA) and run on the following program: holding stage for 2 minutes at 50°C and 10 minutes at 95°C, then the cycling stage for 40 cycles at 95°C for 15 seconds then 1 minute at 60°C. Results were collected by the StepOne software.

Statistical Analysis

Data was analyzed using the statistical software PRISM 7 (GraphPad, San Diego, CA). Analyses were performed using two-tailed unpaired Student's *t*-tests to determine the statistical difference between the injured and control *Abcc6*$^{-/-}$ and WT groups. Results were expressed as means $\pm$ SEM and considered significant for $p < 0.05$.

CHAPTER 3: RESULTS

Specific Aim 1:

Characterize the muscle calcification phenotype by quantifying the amount of calcium and visualizing the phenotype histologically.

Hypothesis:

Abcc6 deficiency causes dystrophic calcification in all muscle tissues, including skeletal muscles.

Preliminary Data

Skeletal Muscle Calcification Phenotype

Previous work in our laboratory studied the role of Abcc6 in the DCC phenotype and demonstrated that supplementation of PPi successfully stopped the progression of cardiac calcification but could not reverse already existing mineralization [33]. The success of these experiments led us to further investigate the acute calcification phenotype in skeletal muscles. We have chosen the gastrocnemius muscle as representative skeletal tissue because it is easily accessible to perform cryoinjury procedures and there is minimal impact on mobility post-surgery. We have also recovered and examined additional skeletal muscles that were injured as part of the DCC process, *i.e.* the incisions made to the abdominal muscles and cryoinjury of the diaphragm (see above description of DCC).

These results (

Figure 7) show increased calcification after cryoinjury to the quadriceps muscle of *Abcc6*$^{-/-}$ mice and mirrored the DCC model in *Abcc6*$^{-/-}$ hearts. This skeletal muscle

dystrophic calcification phenotype was visualized histologically with H&E and Alizarin Red S staining of the injured quadriceps tissues. The injured WT gastrocnemius showed signs of tissue necrosis but there was no evidence of calcification after Alizarin Red staining. However, gastrocnemius tissues from the *Abcc6*$^{-/-}$ mouse showed injury and significant calcification at the area of injury.

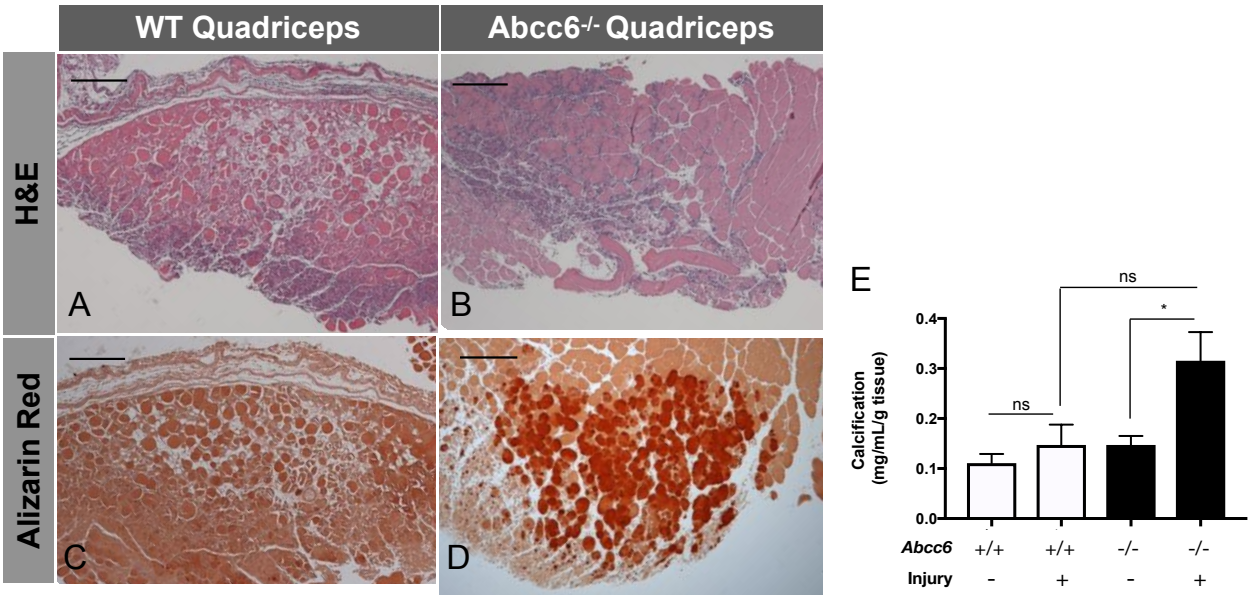

Figure 7: The cryoinjured Abcc6$^{-/-}$ quadriceps (skeletal muscle) with more calcification than WT. *The H&E straining shows necrosis at the site of injury in both strains* **(A,B)**. *The WT quadriceps did not exhibit calcification after injury* ***(C)***, *while the Abcc6$^{-/-}$ quadriceps exhibited significant calcification after injury* ***(D)***. *The significant increase in Abcc6$^{-/-}$ calcification is confirmed by the calcium assay* ***(E)***. *Scale (200 μM).*

Other tissues injured during survival procedures were also harvested for calcification analysis. The diaphragm, suture puncture wounds, and tissue folds of the incision sites in the abdominal area also displayed calcification (Figure 8).

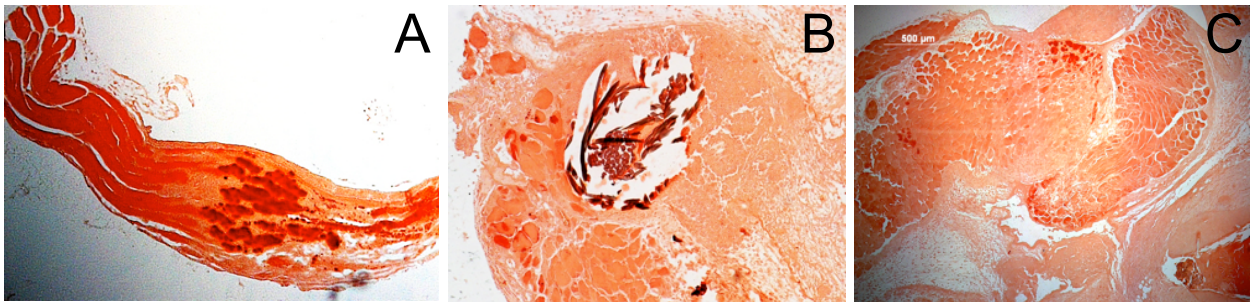

Figure 8: Calcium staining of Abcc6$^{-/-}$ tissues injured in survival surgeries.

*The diaphragm **(A)** is injured during the transdiaphragm heart cryoinjury procedure and calcification is also observed at the puncture injury **(B)** and tissue folds **(C)** when suturing incisions closed.*

Approach and Significance:

The acute DCC phenotype is now well characterized in the cardiac tissue of *Abcc6*$^{-/-}$ mice, but it is not known if this *Abcc6*-dependent calcification response is cardiac specific or affects other types of muscle tissues. To address this hypothesis, a preliminary study was initiated in 2014 in Dr. Le Saux's laboratory related to skeletal muscle. Mouse quadriceps muscle was subjected to cryoinjury for 10 seconds and tissue samples were harvested seven days later for a calcium quantification assay and histology methods for calcium visualization to characterize the phenotype.

The muscle cryoinjury and histological experiments were repeated in 2016 when I joined Dr. Le Saux's laboratory to confirm these initial results. However, after several attempts at reproducing the results, there was no significant difference in calcium levels between the WT control and injured *Abcc6*$^{-/-}$ quadriceps (Figure 10E). It was unclear at the time if the lack of positive results were due to a current technical problem or if the 2014 data were false positives. Therefore, we decided to optimize the skeletal muscle cryoinjury protocol to address this discrepancy.

Attempt to Optimize Cryoinjury Method to Induce Calcification

The goal of adjusting the protocol was to ensure consistency between past and current cryoinjuries as well as tissue collection for calcification assays. First, a suture knot was sewn directly into the muscle to mark the area of injury. The cryoprobe was placed directly on top of the suture to cause injury. This step was important for tissue harvest after the injury has healed as it was much more difficult to visually delineate the injured region from the uninjured one than with cardiac tissues. Moreover, the time of injury was increased from 10 to 30 seconds to cause injury deeper into the muscle and improve the chances of detecting dystrophic calcification. Also, the injury site was changed from the quadriceps to the gastrocnemius because the gastrocnemius muscle had a larger surface area and was easier to access for survival surgeries and tissue harvest. Finally, only 50 μL instead of 200 μL of 0.15 N HCl were added to each sample during the calcium assay to increase the chance of detecting smaller calcium concentration in the supernatant after the 48-hour incubation period.

After repeating our experiments with the adjusted protocol, there was significantly more calcium detected overall, yet the injured gastrocnemius of *Abcc6*$^{-/-}$ mice still did not have higher calcification as compared to the WT (Figure 10F) and no calcification could be visualized histologically in the *Abcc6*$^{-/-}$ gastrocnemius (Figure 10D). Taken altogether, the optimized protocol was only marginally successful in reproducing muscle calcification seen previously.

Histological analyses of additional tissues were carried out when investigating the effectiveness of the optimized protocol. Before discovering the presence of high

concentration of PPi in animal chow, the diaphragm exhibited calcification even when on the high PPi diet.

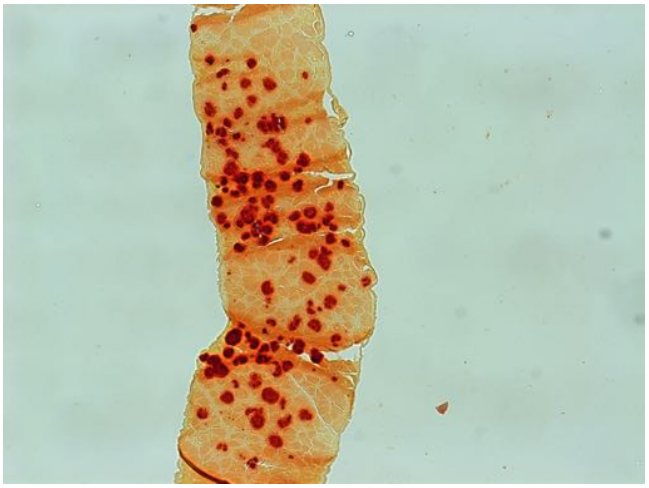

Figure 9: Calcification in the Abcc6$^{-/-}$ diaphragm with high PPi diet .

The Abcc6$^{-/-}$ diaphragm exhibited calcification even when on the high PPi (2920) diet.

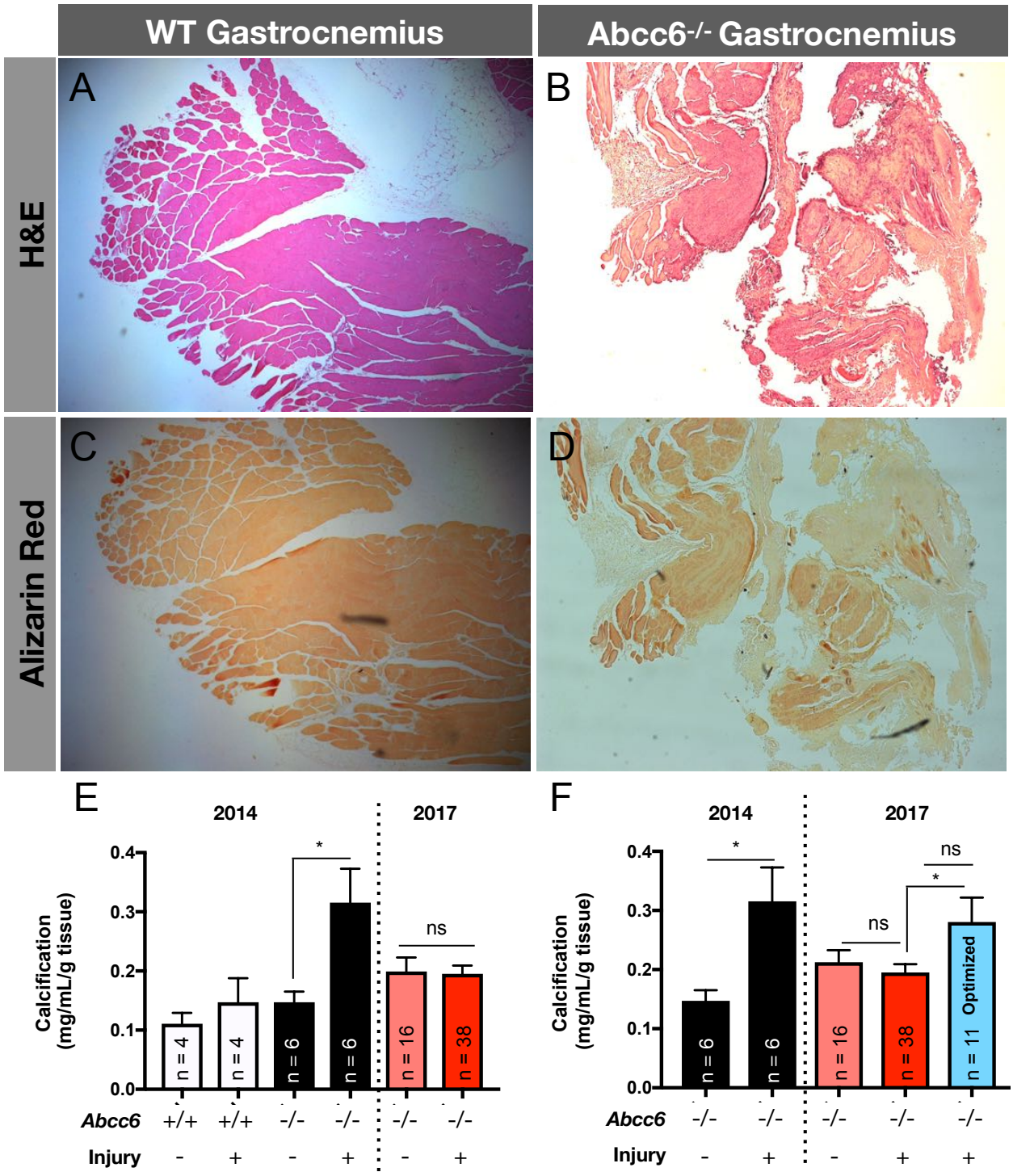

Figure 10: Attempted optimization of cryoinjury protocol only marginally successful with increased calcium quantified in injured Abcc6$^{-/-}$ gastrocnemius but not visualized histologically.

*Attempts at reproducing the preliminary skeletal muscle calcification data were unsuccessful **(E)** and necessitated protocol optimization. However, an increase in Abcc6$^{-/-}$ gastrocnemius calcification could not*

*be visualized histologically despite attempted protocol optimization **(D)**. The altered protocol was marginally successful with an increase in calcium detected, but not to the significant levels initially detected in 2014 **(F)**.*

Exogenous Sources of PPi

Our inability to reproduce the preliminary calcification results of 2014 despite multiple attempts necessitated further investigation. The inconsistency of my results and the inability of Dr. Viola Pomozi - who is an expert in DCC [28, 33] - to induce DCC as part of another project raised the possibility that my results were not necessarily due to technical challenges.

Our laboratory collectively hypothesized that the inhibited calcium development of the well-described acute calcification phenotype in cardiac and skeletal muscle tissues may be related to exogenous factors. The hypothesis of genetic changes or drift in *Abcc6*-/- mice was quickly ruled out since all mice are systematically genotyped. Based on prior published experiments, we have demonstrated that PPi supplementation, even in small or intermittent injection or oral delivery through water, was very effective at suppressing DCC [33, 34]. As PPi contamination either in the water supply or animal was a likely possibility, we developed a protocol to measure the presence of PPi in food, which has never been done before (see Method section).

The PPi levels of the standard rodent diet and water at JABSOM were measured (Figure 11). The PPi content of the water was negligible. Conversely, we found a relatively high PPi content in the current standard chow, designated 2920. Indeed, if one assumes a daily consumption of ~4 g of food for an average mouse of about 25g, and a bioavailability of 0.5% (estimated from intraperitoneal injections), then the average daily

intake of PPi from the current diet would surpass the minimal PPi effective dose (Fig. x red line) previously estimated at ~3.5mg/kg/day [33]. Remarkably, the UH Animal Veterinary Services (AVS) had changed their supplier of animal chow during the second half of 2015. Thus, we further hypothesized that the chow formulation used in 2014 to generate our preliminary results probably contained a lower PPi content. We obtained a sample of animal chow used before 2015 (designated 5053) and measured its PPi content. Even though the food formulations of the pre- and post-2015 diets (5053 *vs* 2920) were comparable (see supplementary data), our results showed that the 5053 diet contained significantly less PPi compared to the post-2015 diet. Importantly, as our method to extract PPi from animal chow is performed in water at 4˚C, it is reasonable to assume that the process is relatively inefficient and the measures of the water supernatant are probably an underestimation.

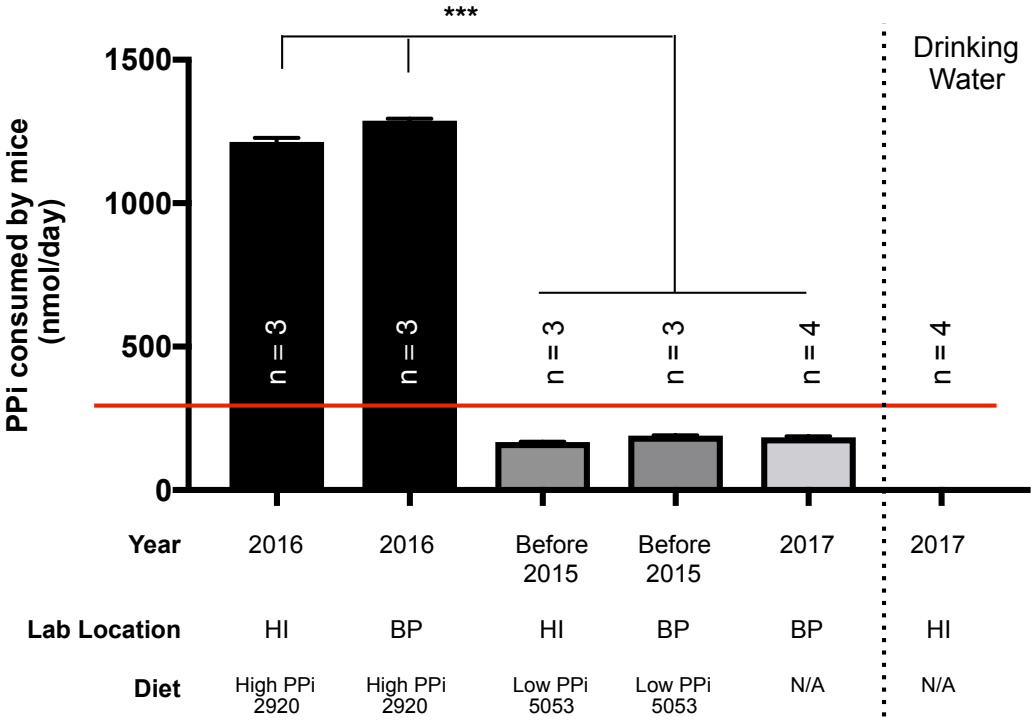

Figure 11: The 2016 rodent diet with a significantly higher concentration of PPi compared to diet used prior to 2015, and nominal PPi content in drinking water.

The chow used in Hawai'i (HI) in 2016 (2920 diet) had significantly higher PPi content than the chow used before 2015 (5053 diet). These results were confirmed by the laboratory's collaborators in Budapest (BP). The standard rodent chow in BP also had significantly lower PPi content than the 2920 diet. The PPi content of the drinking water was negligible.

Moreover, to confirm these results, batches of both the 5053 and 2920 chow were sent to a collaborating investigator (Dr. Varadi) at the Hungarian Academy of Sciences, in Budapest. Dr. Varadi's laboratory obtained similar PPi results (Figure 11). Furthermore, the Budapest group measured the PPi content of the standard rodent chow used at their institution, which was found to have a low PPi concentration like the pre-2015 5053 diet. To further test the hypothesis that the elevated PPi content of the current 2920 diet is indeed capable of inhibiting calcification development in our animal model, we compared calcification in vibrissae of mice on the current 2920 diet and results obtained prior to 2015. As discussed above, the calcification of vibrissae is an effective biomarker to quantify the chronic calcification phenotype in *Abcc6*$^{-/-}$ mice [19]. Vibrissae were harvested from 6 and 12 months old *Abcc6*$^{-/-}$ mice that were born and raised on the 2920 diet rich in PPi and the calcium content was assessed. Our results (

Figure 12) showed that mice fed the high PPi diet (2920) had significantly less calcification in their vibrissae as compared to age-matched *Abcc6*$^{-/-}$ mice raised on the low PPi 5053 diet. These data provided strong evidence linking dietary PPi to lower calcification levels in *Abcc6*$^{-/-}$ mice.

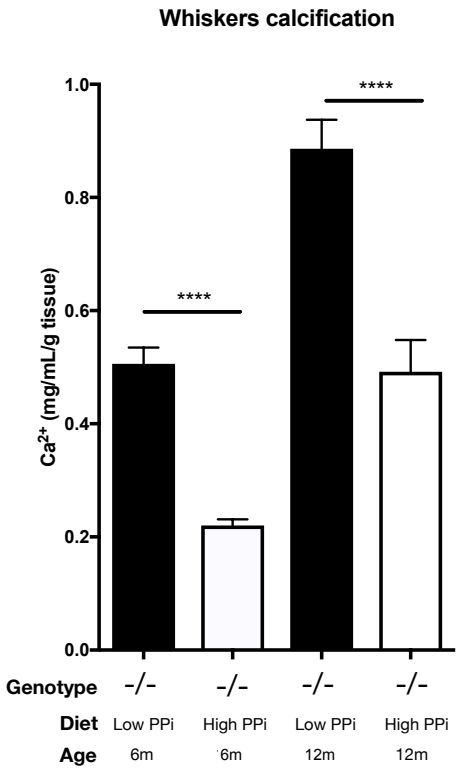

Figure 12: The High PPi diet is linked to reduced Abcc6$^{-/-}$ mice vibrissae calcification.

The 6 month (6m) and 12 month (12m) old mice fed the high PPi diet (2920) had significantly less vibrissae calcification compared to the age-matched Abcc6$^{-/-}$ mice born and raised on the low PPi diet (5053).

Testing the effects of the PPi (2920) diet on *Enpp1*$^{-/-}$ mice.

Our collaboration with Dr. Varadi's laboratory in Hungary allowed us to test the efficacy of the high PPi diet (2920) on *Enpp1*$^{-/-}$ mice, which develop a calcification phenotype similar to *Abcc6*$^{-/-}$ animals at a faster rate beginning *in utero* [34]. Remarkably, the calcification phenotype of *Enpp1*$^{-/-}$ mice is strongly reduced when the animals are supplemented with PPi through water during the perinatal period [34]. The 2920 diet was sent for testing on *Enpp1*$^{-/-}$ mice and preliminary results from Dr. Varadi's laboratory indicate that the 2920 diet significantly reduced vibrissae calcification when provided during the perinatal period (Figure 11).

Reverting to low PPi Diet

Further experiments were done to investigate the effects of dietary PPi on the calcification phenotype. We tested whether substituting the current 2920 high PPi diet for the low PPi 5053 in adult *Abcc6*$^{-/-}$ mice would restore the acute dystrophic calcification phenotype. To test this hypothesis, we procured enough of the low PPi 5053 diet directly from the manufacturer.

Both WT and *Abcc6*$^{-/-}$ mice were put on the low PPi diet for 1 week or up to 1 month. At the end of these periods, mice were subjected to both cardiac and gastrocnemius cryoinjury. Tissues were harvested and excess calcium measured. Unexpectedly, reverting to the low PPi diet for 1 week had an effect opposite to our expectation, *i.e.* the calcification phenotype on both cardiac or gastrocnemius muscles was further reduced (Figure 13). Feeding the mice the low PPi diet for 1 month produced an effect similar to the calcification levels observed in heart tissues after a 1-week period, whereas a non-significant trend upward was noted with the gastrocnemius muscle.

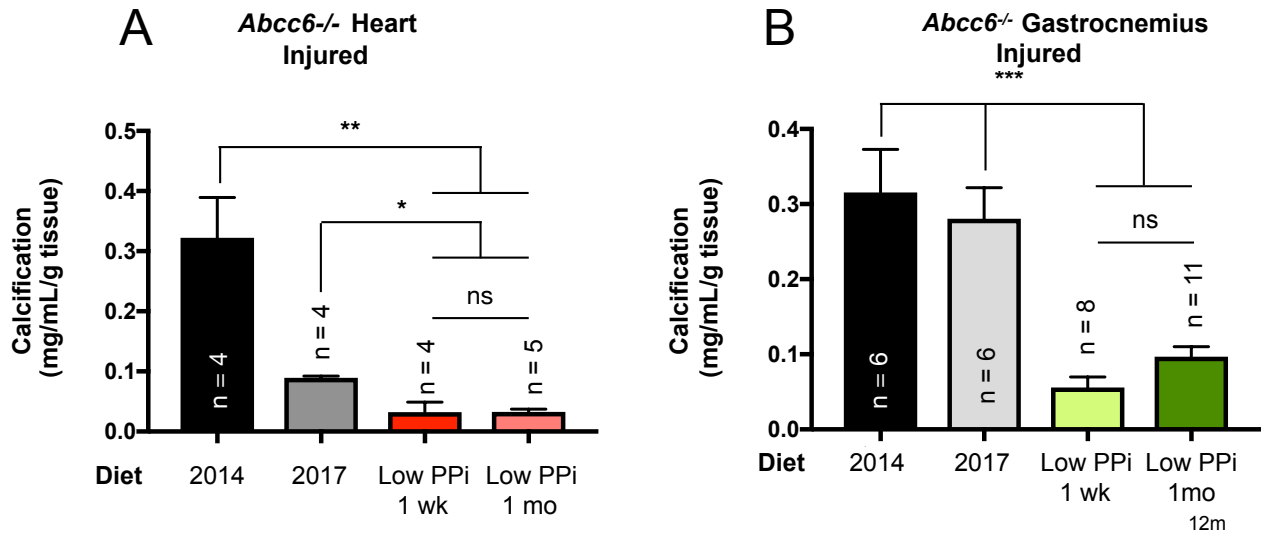

Figure 13: Reverting to the low PPi (5053) diet caused a decrease in Abcc6$^{-/-}$ heart and gastrocnemius calcification.

*Reverting the Abcc6$^{-/-}$ mice to the low PPi (5053) diet for 1 week (1 wk) caused an unexpected further decrease in heart calcification **(A)** and gastrocnemius calcification **(B)**. Neither tissue exhibited increased calcification despite keeping them on the low PPi diet for a longer period of 1 month (1 mo).*

Acceleration Diet

The acceleration diet (Acc) was created and published by another research group at the Department of Dermatology and Cutaneous Biology of Jefferson Medical College [27]. This diet contains specific mineral modifications to induce calcification in an *Abcc6*$^{-/-}$ mouse model. In comparison to the standard rodent diet, the Acc diet has a 2-fold increase in absorbable phosphorus (from 0.43% to 0.85%), a 22-fold increase in vitamin D3 (from 4.4 IU/g to 100 IU/g), and a decrease in calcium (from 1.0% to 0.4%) and magnesium (from 0.22% to 0.04%) [40]. The *Abcc6*$^{-/-}$ mice on this experimental diet demonstrated faster and more pronounced vibrissae mineralization and extensive mineralization of other tissues such as kidneys, lungs, spleen, and the eyes [41]. Of note, lungs generally don't present calcification in *Abcc6*$^{-/-}$ mice fed a normal diet [20] [19], whereas humans only show sub-clinical changes to pulmonary functions [42] and little mineralization [40]

Although the phenotype induced by this Acc diet extends beyond the normal PXE mineralization, we have initiated testing of this diet to promote the development of dystrophic mineralization in our mouse model that (initially) failed to produce gastrocnemius calcification and failed to revert to a calcification-prone phenotype after switching to the 5053 diet.

The same experimental setup was used with WT and* Abcc6$^{-/-}$ *mice that were fed the Acc diet for 1 the Acc diet for 1 week or 1 month. The mice were subjected to both cardiac and skeletal muscle skeletal muscle cryoinjury followed by calcium quantification. Results (

Figure 14) showed that levels of calcification increased in the heart and gastrocnemius but not enough to match the 2014 levels. Interestingly, the WT mice also showed evidence of mineralization despite the presence of a functional* Abcc6 *gene (

Figure 14).

Figure 14: The Acc diet increased calcification in Abcc6-/- and WT mice.

The Acc diet successfully induced calcification in heart ***(A)*** *and gastrocnemius* ***(B)****. However, even WT mice displayed calcification comparable to Abcc6$^{-/-}$ mice.*

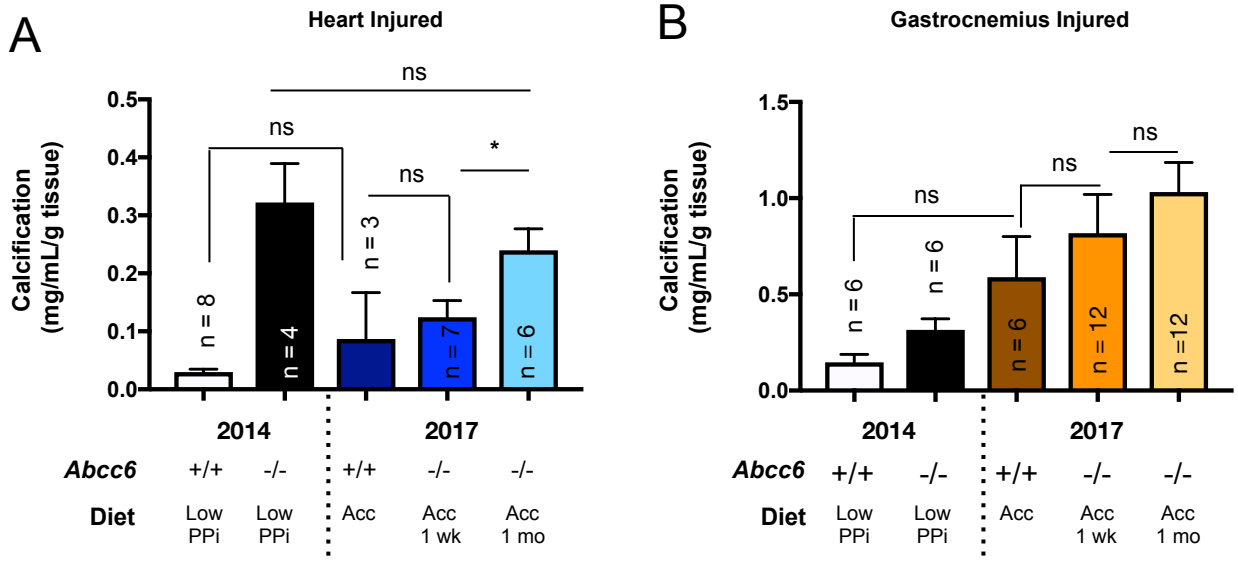

Specific Aim 2:

Explore gene expression and the role of the "Abcc6 pathway" and its molecular players (*Abcc6, Enpp1, Nt5e, Tnap*) in muscle calcification.

Hypothesis:

In the acute calcification phenotype, the lack of Abcc6 lowers ATP efflux and influences the expression of *Enpp1*, *Nt5e,* and *Tnap,* thereby impacting calcification susceptibility.

Approach and Significance

Preliminary Data

Little is known about the gene expression changes that occur in *Abcc6*$^{-/-}$ muscular tissues after dystrophic calcification. Initial gene expression analyses in our laboratory showed that basal levels of *Enpp1* and *Nt5e* expression were decreased in *Abcc6*$^{-/-}$ mice indicating that the absence of Abcc6 function influences gene expression downstream of Abcc6 [33]. Better understanding of the reaction of the molecular pathway downstream of Abcc6 could lead to better interventions to prevent dystrophic calcification in patients with PXE pathologies.

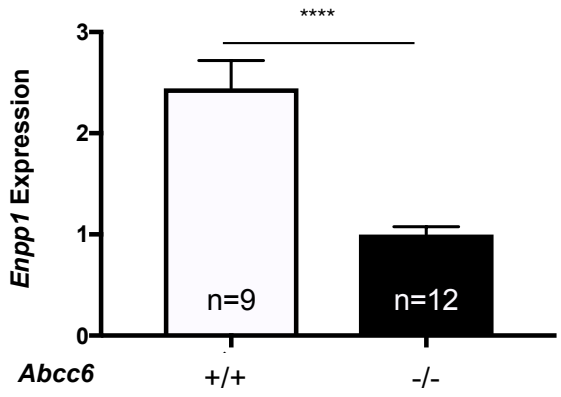

Figure 15: Abcc6$^{-/-}$ livers with lower basal Enpp1 expression.

There is lower expression of Enpp1 in the liver of Abcc6$^{-/-}$ mice compared to WT.

Optimizing Gene Expression Analysis

We initially harvested tissues 7 days after cryoinjury to remain consistent with the DCC protocol and to ensure complete development of calcification. However, as the purpose of this aim was to measure changes in gene expression, it may not necessarily synchronize with calcification.

To test this possibility, heart and gastrocnemius muscles were harvested at 1, 3, and 7-day time points post cryoinjury and *Enpp1* expression was measured. We found

that the expression levels were significantly higher at 3 days post injury in both tissues, though for the heart a *p*-value could not be determined between day 1 and 3 because of the limited samples at day 1 (n=2) (Figure 16). Therefore, all gene expression determinations were performed subsequently 3 days after injury.

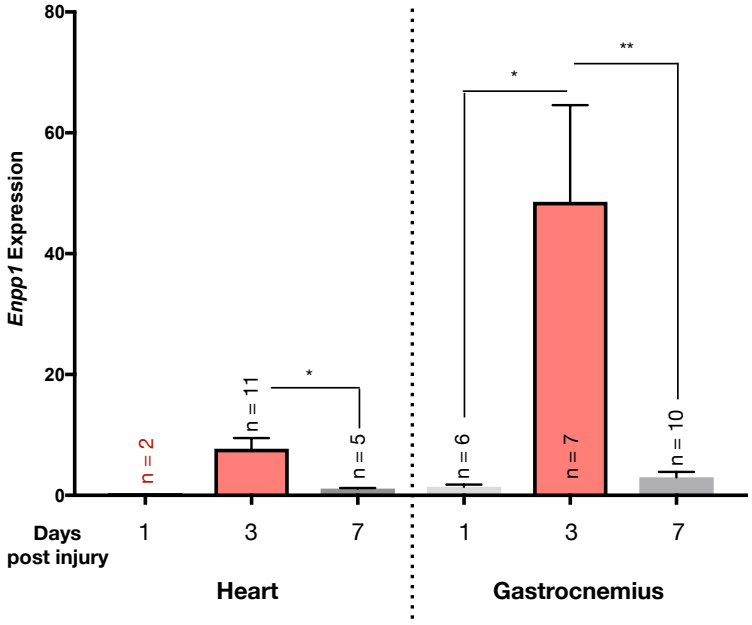

Figure 16: The largest change in gene expression occurs 3 days after injury. *The largest change in Enpp1 expression occurs 3 days after cryoinjury in both the heart and gastrocnemius. At 7 days, the gene expression appears to normalize.*

Gene Expression Results

Both WT and *Abcc6*$^{-/-}$ gastrocnemius and heart exhibited a significant increase in *Enpp1* and *Nt5e* expression specifically after injury (Figure 17). However, at baseline and after injury, there was no significant difference in *Enpp1* or *Nt5e* expression between the WT and *Abcc6*$^{-/-}$ gastrocnemius samples (Figure 17A,C). Conversely, hearts from *Abcc6*$^{-/-}$ mice had significantly higher *Enpp1* expression than the WT hearts 3 days after injury (Figure 17C), while there was no statistically significant difference for *Nt5e* (Figure 17D).

The gene expression changes of *Nt5e* did not fully mirror that of *Enpp1*. In the gastrocnemius, the *Nt5e* expression increased significantly in WT animals after injury, however no significant increase was observed in *Abcc6*$^{-/-}$ mice due to the large variability between individual mice (Figure 17B). There was no significant difference in *Nt5e* expression post injury in WT mice, though we observed a significant rise after injury in *Abcc6*$^{-/-}$ samples (Figure 17D).

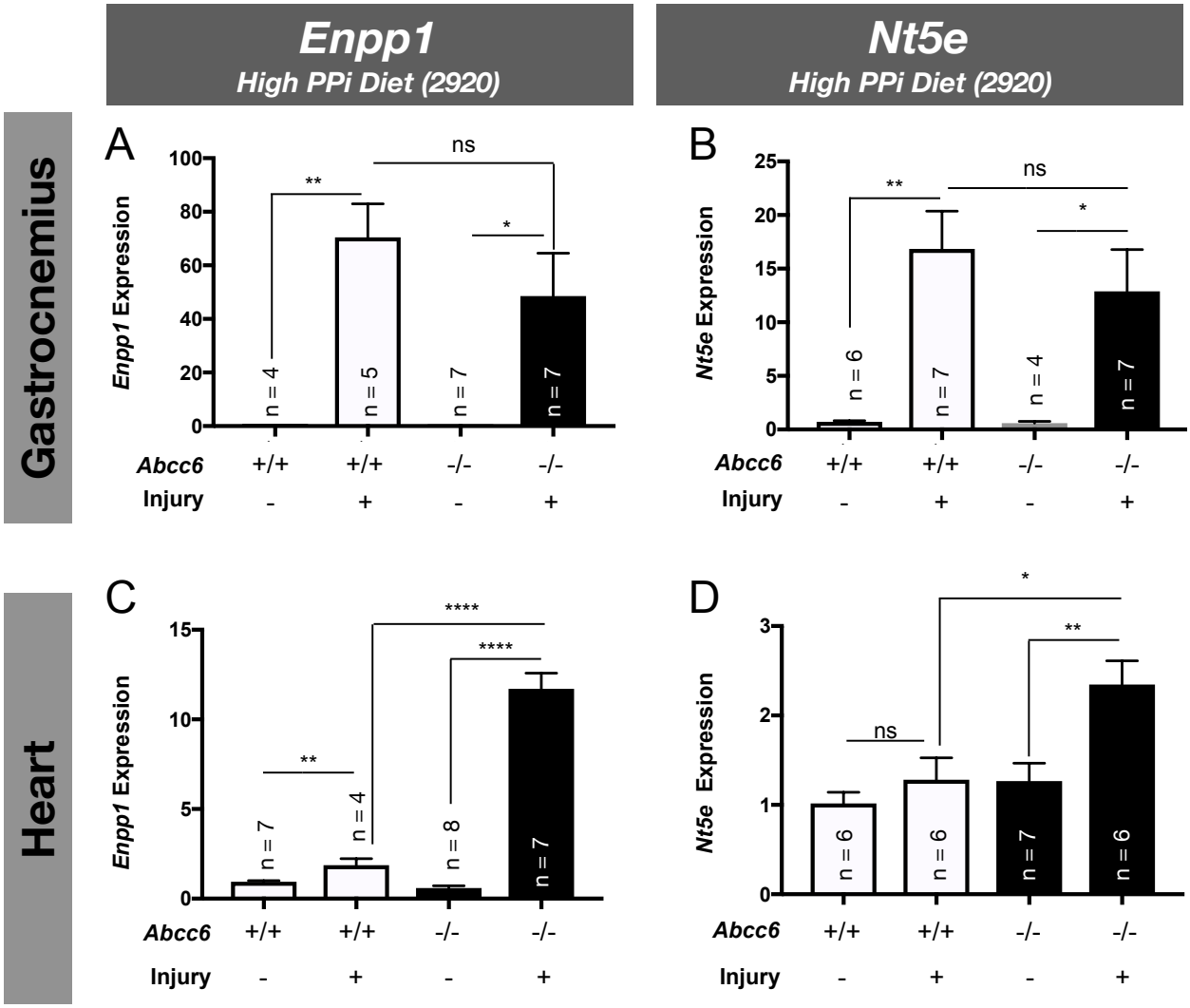

Figure 17: There is positive correlation with Abcc6 in expression of Enpp1 and Nt5e in the heart on the high PPi diet and a trend of increased Enpp1 expression 3 days after injury.

A significant increase of both Enpp1 and Nt5e expression occurs after injury in both the gastrocnemius and heart. The Abcc6$^{-/-}$ hearts have a significantly higher expression of Enpp1 and Nt5e after injury in the heart. No differences in gene expression exist between the injured WT and Abcc6$^{-/-}$ gastrocnemius muscles.

Changes in Gene Expression with the Acceleration Diet

WT and* Abcc6$^{-/-}$ *mice fed the Acc diet for 1 week were also analyzed for gene expression. expression. The diet had no significant effect on* Enpp1 *expression in the gastrocnemius and and heart tissues of WT and* Abcc6$^{-/-}$ *animals (

Figure 18). A* p*-value could not be determined between the control and injured* Abcc6$^{-/-}$ ***gastrocnemius (

Figure 18A) and heart (

Figure 18B) due to limited sample size (n = 2) and (n =0) respectively.

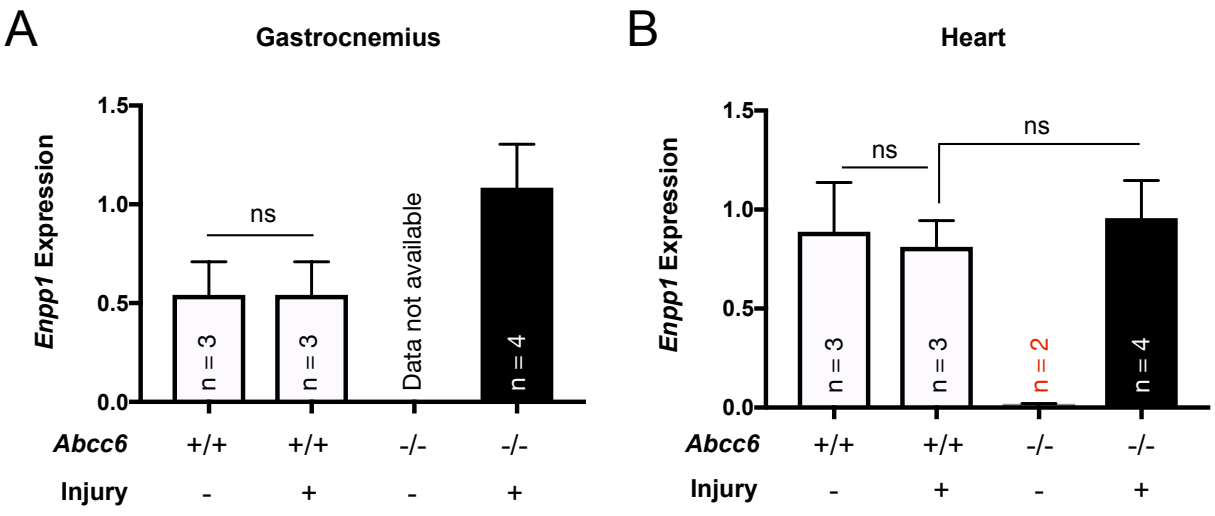

Figure 18: Minimal conclusions could be drawn regarding the impact of the acceleration diet on Enpp1 expression in the heart and gastrocnemius.

There is no significant change in Enpp1 expression between the control and injured WT gastrocnemius ***(A)*** *and hearts* ***(B)****. The limited sample size of the Abcc6$^{-/-}$ injured gastrocnemius and absence of data for Abcc6$^{-/-}$ injured gastrocnemius prevent us from drawing solid conclusions.*

Some *Enpp1* expression experiments were carried out on the diaphragm since histological analysis showed calcification development despite being on the high PPi (2920) diet. However, no significant conclusions could be drawn due to limited sample sizes of WT injured and *Abcc6$^{-/-}$* injured diaphragms (Figure 19).

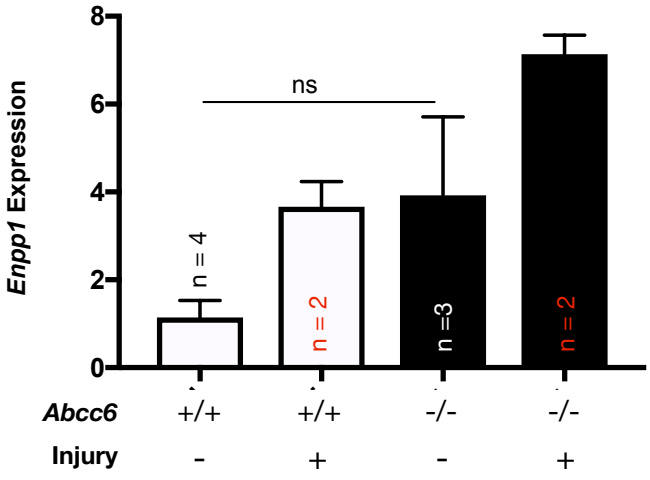

Figure 19: No conclusions could be drawn regarding the impact of the high PPi diet on diaphragm Enpp1 expression.

The p-values could not be calculated due to limited sample sizes (red text).

Specific Aim 3:

Supplementation of PPi to counteract skeletal muscle calcification

Hypothesis:

The supplementation of PPi will reduce the amount of calcification in skeletal muscles.

Approach and Significance

The original approach to investigating this aim was to supplement *Abcc6*$^{-/-}$ mice with PPi. Previous work published by our laboratory demonstrated that PPi supplementation through intraperitoneal (ip) injections prevented chronic and acute calcification in *Abcc6*$^{-/-}$ mice [28]. The difficulties we had in reproducing the acute calcification phenotype in skeletal muscle for Aim 1 (Figure 10) prevented us from conducting the necessary PPi supplementation experiments for this Aim.

Some *Enpp1* expression experiments were conducted to investigate if PPi supplementation impacted gene expression before discovering the presence of a high concentration of PPi in animal chow. These initial results showed that *Enpp1* expression decreased significantly in the *Abcc6*$^{-/-}$ mice supplemented with PPi (Figure 20). Experiments for this aim were discontinued once we determined that the high PPi content of the standard animal diet could have skewed our data.

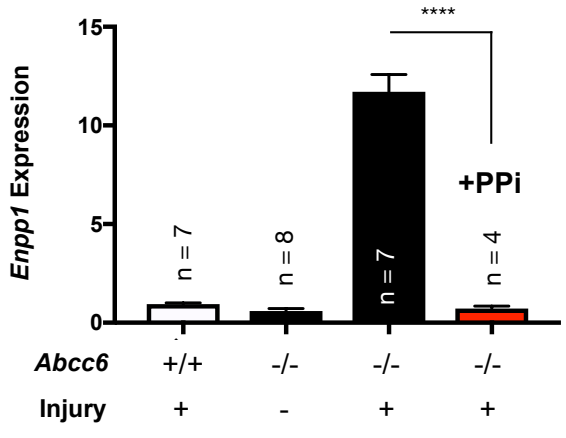

Figure 20: PPi supplementation has a strong attenuate response in heart Enpp1 expression. *The supplementation of PPi via ip injection to Abcc6*$^{-/-}$ *mice after cardiac cryoinjury significantly reduced Enpp1 expression in the heart.*

PPi Through Diet

Although we were unable to formally complete Aim 3, results obtained from the unexpectedly high PPi content of the animal chow from Aim 1 inadvertently provided information on how dietary PPi supplementation impacts the calcification phenotype. The high PPi content of the diet was discovered before conducting experiments for Aim 3 and prevented us from conducting PPi supplementation experiments via ip injection. The investigation of dietary phosphate became the primary focus of my project due to the profound impact it had on my results.

CHAPTER 4: DISCUSSION AND FUTURE DIRECTIONS

The unexpected consequences of dietary PPi on calcification

The initial challenges encountered in reproducing the 2014 gastrocnemius calcification results ultimately altered the course of my original investigation. We identified the exogenous source of PPi as coming from the rodent diet. The results from this aim brought us to four main conclusions:

1. Modest amounts of pyrophosphate found in the diet (Figure 11) has a profound effect on the chronic and acute calcification phenotypes. This was also confirmed with the preliminary results from our collaborators in Budapest with the *Enpp1*$^{-/-}$/tip toe walking (ttw) mice (**Error! Reference source not found.**).

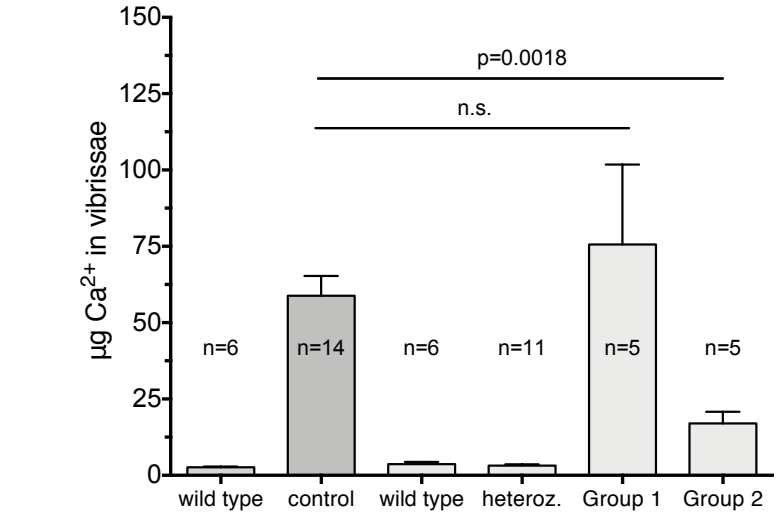

L-PPi = low PPi content Budapest chow
H-PPi = high PPi content Hawaii chow

From Varadi et al (Budapest collaborator), not yet published

Figure 21: Dietary PPi appears to reduce calcification in Enpp1$^{-/-}$ mice(ttw) mice.

Whisker calcification in Enpp1$^{-/-}$ mice. Mice were fed either low PPi diet (L-PPi) from Hungary or the 2920 high PPi chow from Hawai'i (H-PPi). Because Enpp1$^{-/-}$ mice develop most calcification in utero, animals were exposed to control or high PPi chow during pregnancy through weaning.

2. We have already successfully tested PPi supplementation through water and PPi in food may be another possible approach to alleviate or slow the progression of the PXE phenotype in patients through dietary changes. These results suggest dietary intervention may help mitigate pathologic calcification. One could consider consuming foods enriched with PPi or adding "PPi salt" to the diet. The addition of PPi to the diet is being tested in Budapest on healthy subjects and in Finland on PXE patients. PPi is a known additive in commercial food mixes that act as leavening, emulsifiers, and stabilizers important to maintaining quality shelf life of foods [5]. It is also added to flavored milk, cured meats, potato products, and canned fish [5]. High-phosphorus foods include milk products and fast-food products like cheeseburgers.
3. The varying amounts of PPi in food may explain the phenotypic heterogeneity in the PXE phenotype. Previous theories suggested that the lack of correlation between genotype and phenotype and intra-familial variations was due to modifier genes, but this was not proven despite multiple attempts [43-46]. The different phenotypes and different severities in siblings with PXE may be explained by dietary preference.

4. Variations in standard chow between institutions and countries may explain divergent results and lack of reproducibility of results between laboratories. The importance of the *Abcc6*$^{-/-}$ mouse genetic background in PXE is now well understood, while that of the animal chow is not. Our study demonstrated the impact that diet may have on phenotypic outcome and highlights the differences between what is considered "standard chow" across institutions.

It is important to consider the potential impact of genetic drift on the *Abcc6*$^{-/-}$ colony. Variants in the colony may result after 2 to 3 years and could provide a potential explanation as to why the *Abcc6*$^{-/-}$ mice are no longer calcifying after injury as expected.

Although we do not have an idea of how the 2920 diet has become enriched in PPi, we explored the possibility that it may be linked to irradiation of the chow causing the breakdown of polyphosphates or polymerization of monophosphates. The 2020x diet is formulated identically to the 2920 (high PPi), except it is non-irradiated (non-irr). We procured a sample of the 2020x and no significant difference in PPi content was found. The source of PPi is still unknown.

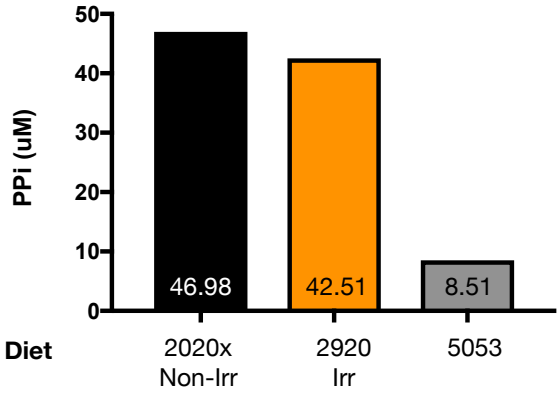

Figure 22: Radiation is not the source of increased PPi in the 2920 diet.

There was no significant difference in PPi content between the irradiated (irr) and non-irradiated (non-irr) foods.

The Acceleration diet may not be an appropriate tool for the *Abcc6*$^{-/-}$ mouse model

The Acc diet was utilized as an attempt to compensate for the lack of positive results during the results during the initial part of the project, before we identified the presence of elevated levels of levels of PPi in the diet. The results showed that, in some cases, even WT mice displayed displayed calcification comparable to* Abcc6$^{-/-}$ *mice (

Figure 14), which suggests the high levels of Vitamin D3 present in this diet may induce acute calcification in muscle tissues in an *Abcc6*-independent manner. Moreover, the Acc diet may not be appropriate to use for dystrophic calcification studies and brings into question the previously published results on the chronic (passive) calcification phenotype [27, 40].

A unique response to injury in the diaphragm

The diaphragm (a smooth muscle) and its response to injury was somewhat different than that of heart and skeletal muscle. The *Abcc6*$^{-/-}$ injured diaphragm exhibited calcification while being exposed to high levels of exogenous PPi in the diet (Figure 19). This suggests that exogenous PPi was less effective in this tissue and that the components of smooth muscle tissues may alter its response to injury. Gene expression showed a similar trend but a small sample size precluded us from establishing a formal conclusion.

Reversion to the low PPi with unexpected results

Changing back to the low PPi diet for short periods of time (1 week to 1 month) did not produce the expected return to higher levels of calcification in response to injury in the gastrocnemius muscle (Figure 13). This suggests that an adaptive mechanism

may be at play and that much more needs to be done to understand the role of PPi in ectopic calcification.

Further molecular characterization of key players in the "ABCC6 pathway"

Previous literature [25] [33] on *Enpp1*$^{-/-}$ mice suggests that the lack of Abcc6 function alters the expression of the genes downstream (*Enpp1, Nt5e, Alpl i.e. Tnap)* in response to tissue injury and may be contributing to the DCC phenotype. The results obtained on *Enpp1* expression in the heart (Figure 20) showed a strong attenuate response (probably product-dependent) to PPi supplementation. This notable change at the molecular level may be linked to the unexpected results of the Aim 1 skeletal muscle calcification phenotype results that were likely skewed due to high levels of dietary PPi. *Enpp1* and *Nt5e* expression in the heart showed a positive correlation with *Abcc6* expression (Figure 17), where the injured *Abcc6*$^{-/-}$ group had significantly higher expression compared to injured WT. These encouraging results of *Enpp1* and *Nt5e* expression in the heart support our hypothesis and experiments will be repeated with the mice being born and raised on the low PPi diet. Although basal levels of *Enpp1* expression were not significantly different in some groups (WT and *Abcc6*$^{-/-}$ gastrocnemius and heart), there is a trend that *Enpp1* expression increases in response to injury. The absence of differences in gene expression between the WT and *Abcc6*$^{-/-}$ mice coincides with the Aim 1 data where the *Abcc6*$^{-/-}$ heart and gastrocnemius tissues did not calcify as we expected (Figure 13), which can be attributed to the increase in PPi in the circulation from the 2920 diet that inhibited calcification. Taken altogether, the absence of calcification and lack of significant changes in gene expression between the

WT and *Abcc6*$^{-/-}$ groups may be attributed to the inhibition of the calcification phenotype by PPi.

As for *Tnap* (*Alpl*), the expression of this gene was low in the heart and skeletal muscles after using two probes, but this is not the first indication of this, as similar results found little expression in cardiac tissues [25]. This suggests that, contrary to what Ziegler et al suggested [26], TNAP in peripheral connective tissues plays a role in the chronic phenotype. This might not be the case for the acute dystrophic calcification phenotype affecting muscular tissues and, therefore, it is probable that Tnap does not play a role in the DCC phenotype.

Conclusion

Overall, the elevated level of PPi in the diet produced valuable data that was just published. However, this prevented us from achieving the goals of the specific aims. Therefore, we intend to repeat many of these experiments with the 5053 diet. Given that reverting to the low PPi diet did not produce the expected rise in calcification post injury, these experiments will be conducted with animals being born and raised on the low PPi diet. The idea of PPi supplementation in humans is also being explored and is currently being tested on healthy subjects in Budapest. What was thought to be an innocuous change in diet formulation had a profound impact on the results and data reproducibility across our entire laboratory. Showing a possible link between dietary PPi and a decrease in calcification opens a new door to study how dietary intervention can be used to control and treat pathologic calcification.

Literature Cited

1. Le Saux, O., et al., *The molecular and physiological roles of ABCC6: more than meets the eye.* Front Genet, 2012. **3**: p. 289.
2. Heinonen, J.K., *Biological role of inorganic pyrophosphate*. 2001, Boston: Kluwer Academic Publishers. viii, 250 p.
3. Boron, W.F. and E.L. Boulpaep, *Medical physiology*. 2017, Elsevier,: Philadelphia, PA. p. 1 online resource (xii, 1297 pages).
4. Boron, W.F. and E.L. Boulpaep, *Medical physiology*. 2015, Elsevier,: Philadelphia, PA. p. 1 online resource (xii, 1297 pages).
5. Renee, J. *The Function of Phosphate*. 2017 [cited 2018 4/11/2018]; Available from: https://www.livestrong.com/article/532554-the-function-of-phosphate/.
6. Alberts, B., *Molecular biology of the cell*. 5th ed. 2008, New York: Garland Science.
7. Varadi, A., et al., *ABCC6 as a target in pseudoxanthoma elasticum.* Curr Drug Targets, 2011. **12**(5): p. 671-82.
8. Beck, K., et al., *The distribution of Abcc6 in normal mouse tissues suggests multiple functions for this ABC transporter.* J Histochem Cytochem, 2003. **51**(7): p. 887-902.
9. Beck, K., et al., *Analysis of ABCC6 (MRP6) in normal human tissues.* Histochem Cell Biol, 2005. **123**(4-5): p. 517-28.
10. Meng, H., et al., *Identification of Abcc6 as the major causal gene for dystrophic cardiac calcification in mice through integrative genomics.* Proc Natl Acad Sci U S A, 2007. **104**(11): p. 4530-5.

11. Jansen, R.S., et al., *ABCC6-mediated ATP secretion by the liver is the main source of the mineralization inhibitor inorganic pyrophosphate in the systemic circulation-brief report.* Arterioscler Thromb Vasc Biol, 2014. **34**(9): p. 1985-9.
12. Washington, D.o.R.U.o. *Soft Tissue Calcifications*. 11/2/17]; Available from: https://rad.washington.edu/about-us/academic-sections/musculoskeletal-radiology/teaching-materials/online-musculoskeletal-radiology-book/soft-tissue-calcifications/.
13. Atzeni, F., P. Sarzi-Puttini, and M. Bevilacqua, *Calcium deposition and associated chronic diseases (atherosclerosis, diffuse idiopathic skeletal hyperostosis, and others).* Rheum Dis Clin North Am, 2006. **32**(2): p. 413-26, viii.
14. Brampton, C., et al., *The level of hepatic ABCC6 expression determines the severity of calcification after cardiac injury.* Am J Pathol, 2014. **184**(1): p. 159-70.
15. (NORD), N.O.f.R.D. *Pseudoxanthoma Elasticum (PXE)*. [Webpage] 2015 [cited 2018 1/31/2018]; Available from: https://rarediseases.org/rare-diseases/pseudoxanthoma-elasticum-pxe/.
16. Le Saux, O., et al., *Mutations in a gene encoding an ABC transporter cause pseudoxanthoma elasticum.* Nat Genet, 2000. **25**(2): p. 223-7.
17. Aiello, C.V., *Multidrug resistance-associated proteins*. 2007, New York: Nova Science Publishers. xii, 251 p.
18. Brampton, C., et al., *Vitamin K does not prevent soft tissue mineralization in a mouse model of pseudoxanthoma elasticum.* Cell Cycle, 2011. **10**(11): p. 1810-20.

19. Klement, J.F., et al., *Targeted ablation of the abcc6 gene results in ectopic mineralization of connective tissues.* Mol Cell Biol, 2005. **25**(18): p. 8299-310.

20. Gorgels, T.G., et al., *Disruption of Abcc6 in the mouse: novel insight in the pathogenesis of pseudoxanthoma elasticum.* Hum Mol Genet, 2005. **14**(13): p. 1763-73.

21. Huesa, C., et al., *Effects of etidronate on the Enpp1(-)/(-) mouse model of generalized arterial calcification of infancy.* Int J Mol Med, 2015. **36**(1): p. 159-65.

22. Nitschke, Y., et al., *Generalized arterial calcification of infancy and pseudoxanthoma elasticum can be caused by mutations in either ENPP1 or ABCC6.* Am J Hum Genet, 2012. **90**(1): p. 25-39.

23. St Hilaire, C., et al., *NT5E mutations and arterial calcifications.* N Engl J Med, 2011. **364**(5): p. 432-42.

24. Markello, T.C., et al., *Vascular pathology of medial arterial calcifications in NT5E deficiency: implications for the role of adenosine in pseudoxanthoma elasticum.* Mol Genet Metab, 2011. **103**(1): p. 44-50.

25. Miglionico, R., et al., *Dysregulation of gene expression in ABCC6 knockdown HepG2 cells.* Cell Mol Biol Lett, 2014. **19**(4): p. 517-26.

26. Ziegler, S.G., et al., *Ectopic calcification in pseudoxanthoma elasticum responds to inhibition of tissue-nonspecific alkaline phosphatase.* Sci Transl Med, 2017. **9**(393).

27. Li, Q., J. Kingman, and J. Uitto, *Mineral content of the maternal diet influences ectopic mineralization in offspring of Abcc6(-/-) mice.* Cell Cycle, 2015. **14**(19): p. 3184-9.

28. Pomozi, V., et al., *Pyrophosphate Supplementation Prevents Chronic and Acute Calcification in ABCC6-Deficient Mice.* Am J Pathol, 2017. **187**(6): p. 1258-1272.

29. Aherrahrou, Z., et al., *An alternative splice variant in Abcc6, the gene causing dystrophic calcification, leads to protein deficiency in C3H/He mice.* J Biol Chem, 2008. **283**(12): p. 7608-15.

30. Ivandic, B.T., et al., *New Dyscalc loci for myocardial cell necrosis and calcification (dystrophic cardiac calcinosis) in mice.* Physiol Genomics, 2001. **6**(3): p. 137-44.

31. Korff, S., et al., *Fine mapping of Dyscalc1, the major genetic determinant of dystrophic cardiac calcification in mice.* Physiol Genomics, 2006. **25**(3): p. 387-92.

32. Ivandic, B.T., et al., *A locus on chromosome 7 determines myocardial cell necrosis and calcification (dystrophic cardiac calcinosis) in mice.* Proc Natl Acad Sci U S A, 1996. **93**(11): p. 5483-8.

33. Pomozi, V., et al., *Functional Rescue of ABCC6 Deficiency by 4-Phenylbutyrate Therapy Reduces Dystrophic Calcification in Abcc6(-/-) Mice.* J Invest Dermatol, 2017. **137**(3): p. 595-602.

34. Dedinszki, D., et al., *Oral administration of pyrophosphate inhibits connective tissue calcification.* EMBO Mol Med, 2017. **9**(11): p. 1463-1470.

35. Russell, R.G., et al., *Inorganic pyrophosphate in plasma in normal persons and in patients with hypophosphatasia, osteogenesis imperfecta, and other disorders of bone.* J Clin Invest, 1971. **50**(5): p. 961-9.

36. Kauffenstein, G., et al., *Alteration of Extracellular Nucleotide Metabolism in Pseudoxanthoma Elasticum.* J Invest Dermatol, 2018.

37. Le Saux, O., et al., *Expression and in vivo rescue of human ABCC6 disease-causing mutants in mouse liver.* PLoS One, 2011. **6**(9): p. e24738.

38. Aherrahrou, Z., et al., *A locus on chromosome 7 determines dramatic up-regulation of osteopontin in dystrophic cardiac calcification in mice.* Am J Pathol, 2004. **164**(4): p. 1379-87.

39. Mc, G.-R.S., *Histochemical methods for calcium.* J Histochem Cytochem, 1958. **6**(1): p. 22-42.

40. Li, Q. and J. Uitto, *The mineralization phenotype in Abcc6 (-/-) mice is affected by Ggcx gene deficiency and genetic background--a model for pseudoxanthoma elasticum.* J Mol Med (Berl), 2010. **88**(2): p. 173-81.

41. Jiang, Q. and J. Uitto, *Restricting dietary magnesium accelerates ectopic connective tissue mineralization in a mouse model of pseudoxanthoma elasticum (Abcc6(-/-)).* Exp Dermatol, 2012. **21**(9): p. 694-9.

42. Pingel, S., et al., *Pseudoxanthoma Elasticum - Also a Lung Disease? The Respiratory Affection of Patients with Pseudoxanthoma Elasticum.* PLoS One, 2016. **11**(9): p. e0162337.

43. Le Saux, O., et al., *A spectrum of ABCC6 mutations is responsible for pseudoxanthoma elasticum.* Am J Hum Genet, 2001. **69**(4): p. 749-64.

44. Hosen, M.J., et al., *Efficiency of exome sequencing for the molecular diagnosis of pseudoxanthoma elasticum.* J Invest Dermatol, 2015. **135**(4): p. 992-998.

45. Hendig, D., C. Knabbe, and C. Gotting, *New insights into the pathogenesis of pseudoxanthoma elasticum and related soft tissue calcification disorders by identifying genetic interactions and modifiers.* Front Genet, 2013. **4**: p. 114.

46. Vanakker, O.M., M.J. Hosen, and A.D. Paepe, *The ABCC6 transporter: what lessons can be learnt from other ATP-binding cassette transporters?* Front Genet, 2013. **4**: p. 203.